

Parametric Hydrogen Tank Sizing Model for Aircraft Conceptual Design

Gala Licheva

**A Thesis
in
The Department
of
Mechanical, Industrial and Aerospace Engineering**

**Presented in Partial Fulfillment of the Requirements
for the Degree of
Master of Applied Science (Mechanical Engineering) at
Concordia University
Montréal, Québec, Canada**

December 2024

© Gala Licheva, 2025

CONCORDIA UNIVERSITY
School of Graduate Studies

This is to certify that the thesis prepared

By: **Gala Licheva**
Entitled: **Parametric Hydrogen Tank Sizing Model for Aircraft Conceptual Design**

and submitted in partial fulfillment of the requirements for the degree of

Master of Applied Science (Mechanical Engineering)

complies with the regulations of this University and meets the accepted standards with respect to originality and quality.

Signed by the Final Examining Committee:

Dr. Charles Basenga Kiyanda Chair

Dr. Frédéric Sirois External Examiner

Dr. Charles Basenga Kiyanda Examiner

Dr. Susan Liscouët-Hanke Supervisor

Approved by _____
Muthukumaran Packirisamy, Chair
Department of Mechanical, Industrial and Aerospace Engineering

_____ 2025

Mourad Debbabi, Dean
Gina Cody School of Engineering and Computer Science

Abstract

Parametric Hydrogen Tank Sizing Model for Aircraft Conceptual Design

Gala Licheva

Hydrogen-based propulsion is a promising research area for reducing aviation's CO₂ emissions. However, hydrogen's low volumetric efficiency makes this alternative fuel challenging in terms of storage and integration into the aircraft. Developing parametric models becomes essential to allow sizing and exploration of possible hydrogen storage tank configurations and layouts within the aircraft. This thesis introduces a model and illustrates analysis capabilities, such as the effect of the variation in geometry on the overall tank volume and mass, which are key aspects to consider in conceptual design. The work presented here combines various methods from the literature into a new parametric approach considering filling and venting pressures, tank geometrical constraints, material properties, and thermal conditions. It supports the analysis of various tank configurations and layouts and allows trade-off studies on gravimetric and volumetric efficiencies to be conducted at the aircraft level. Validation was performed with industry storage tank data and showed an acceptable error range. Case studies illustrate the model capabilities for future hydrogen-powered aircraft configurations. These include tank geometry, thermal insulation, and tank layout-focused studies, allowing the exploration of various aspects of the hydrogen storage system design. Overall, the proposed tank sizing model supports the definition of a feasible design space for future, more environmentally friendly aircraft designs.

Acknowledgments

Completing this thesis has been an enriching experience, one that has brought opportunities, challenges, and growth. Reflecting on this journey fills me with sincere gratitude for the unwavering support, inspiration, and encouragement that has shaped it. This is but a small attempt to express my heartfelt appreciation.

I owe my deepest gratitude to my supervisor, Prof. Susan Liscouët-Hanke, for her advice, encouragement, and guidance. I am thankful for the opportunity to pursue this research and for her invaluable mentorship throughout. Her insights have guided my work and helped me grow both academically and personally, with her dedication being a constant source of inspiration.

I would like to extend my thanks to our industry and academic partners from the EAP project, whose expertise and perspective have enriched my research. The engaging discussions and shared insights have greatly contributed to the development of this work.

I am grateful to my lab mates and dear friends from the Aircraft Systems Lab, who made this experience both memorable and rewarding. Our discussions and shared experiences were truly enriching and cheerful. Their support kept me motivated and made this journey so enjoyable.

A special thanks to my aerospace-and-beyond friends: to Sandrine, who has been by my side from the very beginning of this aerospace engineering journey, offering constant love and support; to Sarah, for her relentless encouragement and for knowing when to take my mind off work and provide moments of lightheartedness; and to Miriam, who, despite being an ocean away, is always there, at any time of the day, ready to support me and remind me that *magic happens*.

Last but not least, thanks to my family, my small group, for their unconditional love and support. They are my source of strength and motivation. No words can express how deeply grateful I am for their constant encouragement and belief in me. I am truly fortunate to have them by my side.

Bringing this work to completion has been a rewarding journey, and I am grateful to all who supported me along the way. Your encouragement, guidance, and support have made all the difference.

Contents

List of Figures	vii
List of Tables	viii
Nomenclature	ix
List of Acronyms	xi
1 Introduction	1
1.1 Background and Motivation	1
1.2 Thesis Scope and Objective	4
1.3 Organization of the Thesis	4
2 Literature Review	5
2.1 Hydrogen Tank Models	5
2.2 Application Cases	6
2.3 Summary and Gap Analysis	7
3 Methodology	12
3.1 Methodology Overview	12
3.2 Required Hydrogen Volume	12
3.2.1 Hydrogen Properties	13
3.2.2 Tank Filling Level	16
3.3 Internal Tank Geometry Sizing	19
3.4 External Tank Geometry Sizing	21
3.4.1 Insulation Materials	21
3.4.2 Insulation Sizing	23
3.5 Methodology Implementation	27
3.6 Hydrogen Tank Sizing Tool Validation	27
3.7 Summary of Chapter 3	29
4 Application Cases	30
4.1 Variation of Tank Geometry	31
4.2 Tank Allocated Space	32
4.3 Tank Sizing Including Insulation	34
4.4 Multiple Tanks with Insulation and Fixed Mass of Hydrogen	37
4.5 Summary of Chapter 4	43

5 Conclusion and Outlook	44
5.1 Contributions	44
5.2 Future Work	45
List of Related Publications	46
References	47
Appendix A Hydrogen Tank Sizing Equations Derivations	51
A.1 Hydrogen Properties	51
A.2 Insulation Sizing	54
Appendix B Insulation Materials Properties	55
Appendix C Tank Geometrical Parameters Solver	56
Appendix D Hydrogen Tank Validation Assumptions	60
Appendix E Tank Layouts Characteristics Data	61

List of Figures

Figure 1.1	Gravimetric and volumetric densities for several fuels	2
Figure 1.2	Cryoplane hydrogen-powered aircraft concepts	3
Figure 1.3	Airbus ZEROe concepts	3
Figure 3.1	Methodology overview	13
Figure 3.2	Density as a function of pressure of hydrogen gas and liquid	14
Figure 3.3	P- ν curve and parameters definitions	15
Figure 3.4	Average density of hydrogen at various volume fractions	16
Figure 3.5	Relationship between the average density and the filling and venting pressures	17
Figure 3.6	Liquid volume fraction with respect to various fill and venting pressures	18
Figure 3.7	Liquid volume fraction for given venting and filling pressures	18
Figure 3.8	Geometrical representation of a modelled tank	19
Figure 3.9	Variation of tank shape with varying geometrical parameters	20
Figure 3.10	Insulation materials properties	22
Figure 3.11	Insulation materials properties in vacuum	23
Figure 3.12	Overview of different insulation types	23
Figure 3.13	Schematic of different insulation types models	25
Figure 3.14	Tool code modules overview	27
Figure 3.15	Comparison of calculated tank mass with data from industry	28
Figure 4.1	Tank sizing model application scenarios	30
Figure 4.2	Impact of geometrical ratios on the tank mass (excluding insulation)	31
Figure 4.3	Impact of geometrical ratios on the tank mass (excluding insulation) - focus on $\phi = 1$	32
Figure 4.4	Tank of various shapes in a pre-defined allocated volume	32
Figure 4.5	Impact of tank shape variation on the mass and gravimetric and volumetric efficiencies	33
Figure 4.6	Tank and insulation mass for different insulation materials	35
Figure 4.7	Fuselage cross-section with inserted hydrogen tank	35
Figure 4.8	Impact of exposure time on insulation and tank sizing	36
Figure 4.9	Tank and insulation mass for varying exposure time (for different insulation materials)	36
Figure 4.10	Notional layout of next-generation aircraft architectures	37
Figure 4.11	Hydrogen tanks placement configurations	38
Figure 4.12	Illustration of notional engine rotor burst zone	39
Figure 4.13	Tank and insulation weight for different tank layouts	42

List of Tables

Table 1.1	Comparison of physical storage conditions for hydrogen	2
Table 2.1	Literature review overview table - Research scope	8
Table 2.2	Literature review overview table - Tank structure	9
Table 2.3	Literature review overview table - Insulation	10
Table 3.1	Definition of tank geometrical parameters	19
Table 3.2	Insulation types characteristics overview	21
Table 4.1	Assumptions in geometry variation study	31
Table 4.2	Assumptions in tank allocated space study	34
Table 4.3	Assumptions in tank sizing with insulation study	34
Table 4.4	Explored layouts definitions	39
Table 4.5	Assumptions in multiple tank layouts study	40
Table 4.6	Preferred tank configurations based on various selection criteria	41
Table B.1	Insulation materials properties	55
Table D.1	Geometrical parameters for cryogenic tanks	60
Table D.2	Material properties for the validation cases	60
Table D.3	Hydrogen conditions for the validation cases	60
Table E.1	Tank integration characteristics for 50 kg mass of hydrogen	62
Table E.2	Tank integration characteristics for 345 kg mass of hydrogen	63
Table E.3	Tank integration characteristics for 1000 kg mass of hydrogen	64

Nomenclature

Capitals

A	[m ²]	area
E	[Pa]	Young's modulus
K	[Pa]	stress
L	[m]	characteristic length
P	[Pa]	pressure
Q	[J]	heat
\dot{Q}	[J/s]	heat transfer rate
R	[K/W]	thermal resistance
T	[K]	temperature
V	[m ³]	volume

Lower Case Letters

a	[m]	semi-major axis of an ellipse
b	[m]	semi-minor axis (of tank's heads)
c	[m]	semi-minor axis of an ellipse
g	[m/s ²]	gravitational force
h	[W/(m ² · K)]	convection heat transfer coefficient
k	[W/(m · K)]	thermal conductivity
l	[m]	length
m	[kg]	mass
s	[m]	thickness

x	quality, ratio of saturated vapor mass to total mass
y	ratio of volume of liquid to total volume

Symbols

β	[K ⁻¹]	volumetric thermal expansion coefficient
λ		ratio of length of shell tank to total length
ν	[m ³ /kg]	specific volume
ϕ		ratio of a over c
ψ		ratio of b over c
ρ	[kg/m ³]	density
σ	[W/(m ² · K ⁴)]	Stefan-Boltzmann constant (5.67×10^{-8})
ε		emissivity

Subscripts

<i>avg</i>	average
<i>env</i>	environment
<i>f</i>	liquid
<i>fill</i>	filling
<i>g</i>	gas
<i>ins</i>	insulation
<i>op</i>	operating
<i>out</i>	outside
<i>s</i>	shell
<i>sur</i>	surface
<i>t</i>	total
<i>vac</i>	vacuum
<i>vent</i>	venting
<i>w</i>	wall

List of Acronyms

AEB	Aft Equipment Bay
APU	Auxiliary Power Unit
ASME	American Society of Mechanical Engineers
CG	Center of Gravity
EAP	Exploration and modeling of Alternative Propulsion technologies for business jets
EPS	Expanded Polystyrene
LCA	Life-Cycle Assessment
MDAO	Multidisciplinary Design Analysis and Optimization
MLI	Multi-Layer Insulation

Chapter 1

Introduction

Air passenger and freight traffic are both projected to more than double over the next two decades [1], raising concerns about the future environmental impact of the aviation industry. In response, stakeholders have committed to reducing aviation’s environmental impact and reaching carbon neutrality in the next few decades [2]. Exploring new aircraft configurations and technologies is essential in the aim of reaching this target while enabling sustainable development. This chapter outlines the background and motivation driving the research work in this thesis and presents its scope and objectives.

1.1 Background and Motivation

The aviation industry has set a goal to achieve net zero carbon emissions by the year 2050 [2]. Developing breakthrough technologies is essential to ensure the competitive advantage of future aircraft in terms of energy efficiency and environmental impact. This entails integrating advanced technology concepts and adopting cleaner and more sustainable energy sources [3]. Aviation stakeholders are working on the development and implementation of alternative propulsion technologies to reduce their carbon footprint. One of the key initiatives and research avenues toward alternative propulsion and reduction of fossil fuel burn is hydrogen-based propulsion. Hydrogen can be utilized in two main ways: through direct combustion, burned like a conventional fuel to power an engine, or through fuel cell propulsion, used to react with oxygen and produce electricity to drive an electric motor. The challenge with hydrogen-based propulsion lies in the integration and storage of hydrogen within the aircraft.

Hydrogen storage is a key aspect and one of the main challenges in the advancement of hydrogen-based propulsion technologies. Hydrogen has a high energy density, meaning it has a high energy per mass ratio compared to other fuels (see figure 1.1) [4]. Yet, it also has a very low volumetric density at standard atmospheric conditions and, therefore, requires the usage of storage methods allowing for higher energy density. Hydrogen storage comprises two main types: physical-based and material-based storage [4]. Physical storage can be compressed, cryo-compressed, or liquid hydrogen in a vessel. Material-based storage uses adsorption materials, metal hybrids (hydrogen is stored on solids’ surfaces by adsorption or within solids by absorption) or the conversion of hydrogen to different chemical compounds [5]. These latter storage methods are, however, impractical for aeronautics applications because of their excessive weight and volume [6], [7], their complexity or not complete reversibility to pure hydrogen [5]. Table 1.1 compares the different physical-based storage methods for hydrogen. The volume, as well as the safety challenges associated with high-pressure

storage, make gaseous hydrogen a less suitable option for aircraft applications [6].

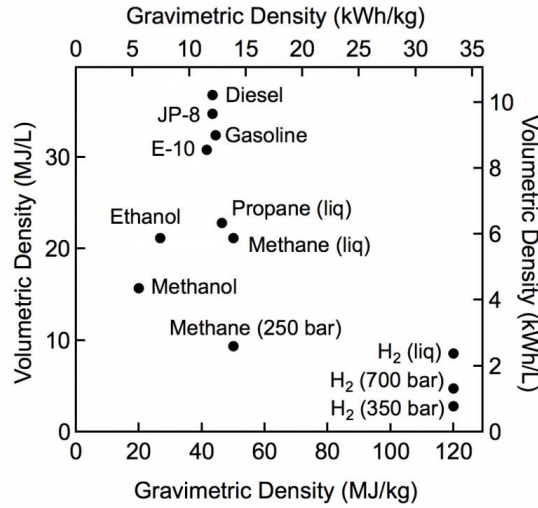


Figure 1.1: Gravimetric and volumetric densities for several fuels [4]

Table 1.1: Comparison of physical storage conditions for hydrogen (adapted from [5], [8], [9], [10])

Form of storage	Temperature [°C]	Pressure [bar]	Density [kg/m ³]	State	Features
Compressed	20	350 or 700	25 to 40	Gaseous	low quantities
Cryo-compressed	-233	350	80	Gaseous	high quantities, heavy
Liquid	-253	3 to 5	71	Liquid	high quantities, low pressure

Liquid hydrogen has a specific energy of 120 MJ/kg and an energy density of 8.5 MJ/L, while conventional fuel has a specific energy of 43.2 MJ/kg and an energy density of 34.9 MJ/L [8], [11]. This makes the energy per unit mass of hydrogen around three times greater than that of conventional fuel. However, its energy density is nearly four times lower, which leads to it taking four times more volume for the same amount of stored energy.

Taking significantly more space than kerosene, storing hydrogen onboard an aircraft is challenging as space within the airframe is highly optimized and very limited. Unlike kerosene, which is traditionally stored in the wings or other compact compartments, hydrogen requires tanks that must be maintained at a certain temperature and pressure to ensure the safety and stability of the system. Storing hydrogen in a liquid form requires maintaining cryogenic temperatures, resulting in complex insulation necessary to prevent heat flow into the tank and minimize boil-off. These insulation systems are generally bulky and heavy, introducing further design and weight challenges. Additionally, larger tanks can impact the aerodynamics and the weight distribution of the aircraft, possibly requiring design modifications. This need for a larger storage volume, along with the integration of more complex insulation to prevent boil-off, adds to the space constraints and challenges of using hydrogen for aviation propulsion.

Hydrogen-powered aircraft concepts have been studied in the past. Studies performed by Lockheed and NASA [12], [13] have assessed the feasibility of liquid hydrogen as aviation fuel for

passenger aircraft. The international project Cryoplane was the first larger-scale project to investigate the possibility of using hydrogen for propulsion with the goal of reducing climate impact [14]. Configuration studies were done on the Airbus 310 as the baseline aircraft and fuselage-top-mounted tanks were deemed the most favourable solution for this type of aircraft. The Tupolev TU-154, a three turbofan engines aircraft, was selected as a baseline aircraft for the development of an experimental aircraft (the TU-155) in which the right-hand side engine and fuel system were modified to operate on liquid hydrogen [15]. Figure 1.2 shows these aircraft configurations studied in the Cryoplane project.

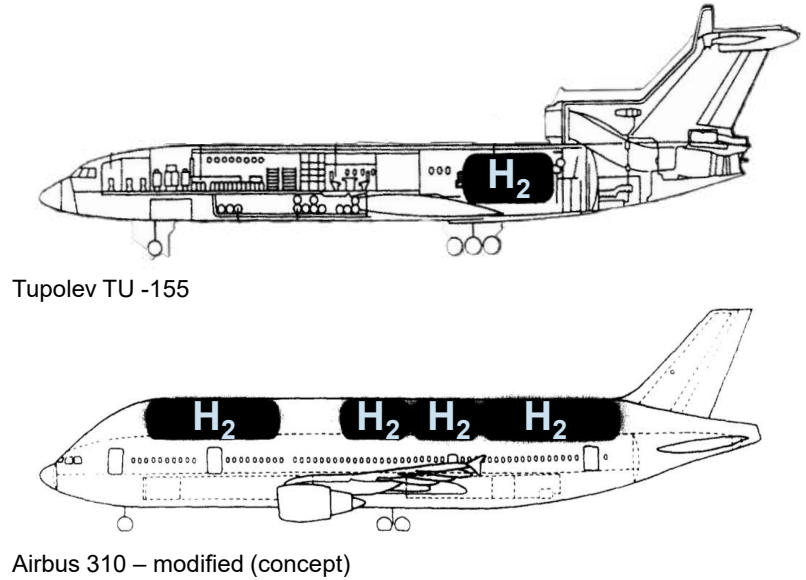


Figure 1.2: Cryoplane hydrogen-powered aircraft concept (adapted from [15])

In recent years, hydrogen propulsion has gained traction again in the aviation industry. ZeroAvia is working on retrofitting turboprop aircraft with fuel cell-based propulsion systems for regional aviation [16]. Airbus announced their ZEROe project aiming to develop three commercial aircraft concepts (a turbofan 1.3a, a turboprop 1.3b and a blended-wing body 1.3c designs) using hydrogen as primary power source [17].



Figure 1.3: Airbus ZEROe concepts [17]

When it comes to hydrogen-based propulsion, the focus is mainly on large commercial aircraft, which have more storage potential due to their relatively large size or, in the case of small fuel-cell

technology demonstrators, on small lower performance aircraft. The project, which this thesis is part of ([Exploration and modeling of Alternative Propulsion technologies for business jets \(EAP\) \[18\]](#)), focuses on business aircraft, which present their own set of challenges when it comes to hydrogen-based propulsion; they are smaller and therefore have less space to accommodate hydrogen tanks, while also having higher performance constraints, such as long-range, high-altitude, and high-speed cruise. The work done as part of this project aims to address these challenges and conduct studies on the feasibility of hydrogen for business jets and the impact on aircraft performance.

In an attempt to explore and evaluate the feasibility and integration of hydrogen-based propulsion systems for aircraft, there is a need to develop models for the design and sizing of hydrogen storage tanks. Parametric models would facilitate this sizing process while considering the various design requirements (i.e., safety and operational requirements). In fact, operational constraints such as tank filling and design venting pressures, ground operation or holding time, and environmental conditions impact the tank sizing and insulation requirements, contributing to the overall mass and volume of the storage system. On the aircraft level, the overall impact of the integration of a new system on the drag and weight needs to be considered and minimized while also considering placement safety constraints, such as rotor burst zones. Consequently, a highly flexible parametric tank sizing model is essential to explore various tank sizes and placements. This model would enable the evaluation of different tank configurations and layouts, allowing for the integration of hydrogen storage tanks meeting specific design and performance requirements and further exploration in an aircraft-level [Multidisciplinary Design Analysis and Optimization \(MDAO\)](#) context.

1.2 Thesis Scope and Objective

The objectives of this thesis are the following:

- Development of a methodology to size tanks with various geometries
- Development of a methodology to size the insulation of the tank to maintain the fluid stored at cryogenic temperatures
- Identification of the parameters influencing the tank sizing
- Development of a code supporting the variation of design parameters

1.3 Organization of the Thesis

The organization of the presented work is the following:

Chapter 2 provides a literature review of the work carried out on cryogenic tank models and application case studies involving hydrogen tanks. Chapter 3 addresses the gaps identified in Chapter 2 and describes the methodology developed to parametrically size cryogenic hydrogen tanks, both internally and externally. The validation of the described methodology is also presented. Chapter 4 demonstrates the use of the developed tool by carrying out various application cases. Finally, Chapter 5 provides a summary and conclusions and discusses future work to further develop the tool's capabilities.

Chapter 2

Literature Review

As mentioned in Chapter 1, hydrogen-based propulsion introduces new challenges in terms of energy storage. The hydrogen needs not only to be stored in sufficient quantities for the aircraft's mission but also in favourable conditions. Different hydrogen storage methods are briefly presented here. Models are developed to allow the exploration of different characteristics of hydrogen storage tanks and their insulation. This section also provides an overview of the work done on hydrogen tank modelling and of case studies of hydrogen tank applications in aviation. It explores the studies done on the tank, system, and aircraft levels. Finally, the main tank characteristics of each study and the research gap are discussed.

2.1 Hydrogen Tank Models

The literature provides several studies and models on cryogenic hydrogen storage technologies, summarized in table 2.1. For the hydrogen to remain in a liquid phase, an insulation allowing it to be maintained at cryogenic temperatures has to be integrated. Models are developed to allow the exploration of different characteristics of hydrogen storage tanks and their insulation. Generally, hydrogen models encompass three aspects: geometrical, mechanical, and thermal. First, the volume and geometry of the tank have to be determined. The mechanical model concerns the thickness of the tank walls and their materials (detailed in table 2.2). Finally, thermal modelling considers the temperatures involved in the storage of hydrogen and its surroundings and the insulation needed to keep it at the desired temperature, the details of which are given in table 2.3.

Brewer [6] lays out the basics of integrating hydrogen technologies in aviation and presents a detailed review of the different components of the fuel containment system and design considerations. The author discusses and compares the main types of tanks (integral and non-integral). The tank's volume is determined based on the amount of hydrogen it needs to carry, plus some allowance for the difference in tank dimensions at different temperatures. This textbook also lists the structural design criteria, i.e. the pressures and stresses the tank will be subjected to. The design criteria for insulation are also explored, and a screening of active (requiring inert gas purging or dynamic pumping to achieve vacuum) and passive concepts for insulation systems is performed. The most promising concepts for use with integral and non-integral tanks are selected for a more detailed analysis and comparison.

Building on [6], several researchers have studied or developed models for hydrogen tanks. Verstraete [19] compares non-integral and integral hydrogen tank concepts and develops a model for integral cylindrical tanks. The author discusses the main challenges in the selection of tank wall

materials and applies the [American Society of Mechanical Engineers \(ASME\)](#) Boiler and Pressure Vessel Code in the sizing of the tank walls. Furthermore, Verstraete considers the pressure fluctuations inside the tank, as well as the filling and venting pressure in the sizing process. A discussion of the different insulation configuration types (internal and external insulation) led to the selection of the external insulation concept. Subsequently, several insulation means were compared: foams, aerogels, vacuum, and [Multi-Layer Insulation \(MLI\)](#). In addition, the thermal considerations for the insulation sizing are discussed. A thermal model for the tank is developed, taking into account the heat conduction through the insulation and the convection inside and outside of the tank. Verstraete also studies the influence of the aircraft mission on the tank design for regional and long-range aircraft. Using this model, in [20], Verstraete et al. study the impact of the tank size and the on-ground hold period on different tank insulation, such as foam and [MLI](#). The sensitivity of the tank weight and size to design parameters, such as the fuselage diameter and the fuel load, is also assessed for regional and long-range aircraft.

Following Verstraete's filling and venting pressure considerations, Winnefeld et al. [21] create a non-integral tank design model featuring ellipsoidal heads and elliptical shells, making the tank more versatile. This design model considers the geometrical, mechanical, and thermal aspects of the hydrogen tank design. A mathematical parametric description of the tank geometry ensures a flexible geometric design. The thermal design of the tank encompasses convective heat transfer at the inner and outer tank surfaces, conduction through the insulation and tank wall, and radiation on the outside of the tank. With the developed model, the authors investigate the dependency between various tank parameters by carrying out geometrical parameter variations. The impact of the distribution of the stored hydrogen in multiple tanks is also explored.

2.2 Application Cases

Building on the models developed by Verstraete and Winnefeld et al., other researchers have conducted studies on hydrogen storage. Mantzaroudis and Theotokoglou [22] look at the temperature distribution through the tank and study the variation of geometrical parameters. They use the Von Mises stress criterion to observe the structural behaviour of the inner shell of the tank and study the relationship between different tank geometrical parameters and the tank's mass. Palladino et al. [23] explore hybrid-electric propulsion architectures, including hydrogen fuel cells for regional aircraft. Parametric studies on the impact of these architectures, and more specifically of the design range and electrical power, on the overall performance of the hybrid aircraft are done.

The following works focus on different aspects of hydrogen tank design and its integration in an aircraft. On the tank level, Colozza et al. [24] explore how the total mass of the tank is affected by the amount of insulation on the tank. They also look at the relationship between the tank system mass and the tank volume. Gomez and Smith [25] investigate the implementation of hydrogen fuel tanks in commercial airplanes according to two different layouts and perform a detailed structural analysis of the different tanks in these layouts. Shank et al. [26] focus on the insulation of the tank and adopt a given geometry for cylindrical and spherical tanks at different conditions, namely on ground and in-flight conditions, and compare different insulation materials applied to these different tanks. Sarkar et al. [27] look at the impact of hydrogen propulsion at the fuel system level. They study a cryogenic fuel system for a narrow-body aircraft for a given mission profile for different insulation thicknesses and times of the day.

Several studies also explore different aspects of the impact of hydrogen-based propulsion on the aircraft level. Onorato et al. [28] study different tank layouts for commercial aircraft and focus on

the pressure profile of the tank and the overall impact of the fuel system on the aircraft in terms of performance compared to a conventionally powered aircraft. Finally, Alsamri et al. [29] perform an analysis of the performance and emissions trade-offs for a business jet retrofitted with a hydrogen-powered fuel cell and discuss the sizing and placement of the hydrogen tanks.

2.3 Summary and Gap Analysis

Tables 2.1 to 2.3 summarize the literature review by providing an overview of the research scope (Table 2.1), the characteristics of the tanks (Table 2.2), and their associated insulation (Table 2.3). In summary, the existing literature provides equations and applications for different tank geometries, materials, and insulation. As table 2.2 reveals, the literature mainly presents studies made on cylindrical tanks and pre-defined tank configurations (with the exception of Winnefeld et al. [21], who developed a parametric tank model) and without addressing the safety considerations of the layout of the tanks within the aircraft. Furthermore, the models developed in the literature take the filling level of the tank into account but lack details on how to calculate the different allowance percentages at venting pressure. This thesis shows, therefore, the steps to a generalized approach for considering different boil-off percentage allowances and attempts to address tanks with more versatile elliptical shapes. Table 2.3 shows that the majority of the surveyed literature does not address the time during which the cryogenic tank would be exposed to the hotter environment. Additionally, for most studies, only one insulation material is considered in the thermal analysis. This thesis attempts to address this gap by surveying different insulation materials for different conditions. Furthermore, in light of the need for safety considerations, the tool proposed here enables the exploration of different layouts and tank gravimetric efficiencies. The presented tool aims to explore the integration of tanks of various shapes and possible placements within the aircraft.

In summary, the proposed methodology in this thesis addresses the following gaps:

- Develop a parametric geometrical tank definition supporting a variety of tank shapes
- Take into consideration different boil-off allowance percentages and provide equations to calculate the effect on the required tank volume
- Take into consideration the exposure time of the tank to the external environment
- Explore different tank insulation materials and their impact on the overall tank sizing
- Address possible tank layout configurations within the aircraft

Table 2.1: Literature review overview table - Research scope

Ref.	Research Focus	Safety Considerations	Layout Considerations	Study Scope
Verstraete (2009) [19]	<ul style="list-style-type: none"> • gravimetric efficiency vs. tank venting pressure • tank length vs. tank venting pressure 	-	yes	Aircraft level
Verstraete et al. (2010) [20]	<ul style="list-style-type: none"> • study the impact of the tank size and the on-ground hold period on different tank insulation; foam, and MLI • sensitivity of the tank weight and size to design parameters, such as the fuselage diameter and the fuel load 	-	yes	Aircraft level
Winnefeld et al. (2018) [21]	<ul style="list-style-type: none"> • relationship between the storage density and different geometry parameters • relationship between the different geometrical parameters and mass and insulation thickness 	-	-	Tank level
Mantzaroudis and Theotokoglou (2023) [22]	<ul style="list-style-type: none"> • temperature distribution through the tank • variation of geometrical parameters and impact on the other parameters, and mass 	-	-	Tank level
Palladino et al. (2021) [23]	<ul style="list-style-type: none"> • exploration of the potential of hybrid-electric propulsion with fuel cells • parametric studies on the impact of the design range and electrical power of the system on the hybrid aircraft performance 	-	-	Aircraft level
Colozza et al. (2002) [24]	<ul style="list-style-type: none"> • effect of insulation thickness on overall tank system weight (system mass vs. thickness) • tank system mass as a percent of usable liquid hydrogen (tank system mass as a % of total hydrogen mass vs. tank volume) 	-	-	Tank level
Gomez and Smith (2019) [25]	structural stress analysis	-	-	Tank level
Shank et al. (2023) [26]	<ul style="list-style-type: none"> • comparing spherical vs. cylindrical shapes • comparing different insulation materials at different conditions 	-	-	Tank level
Sarkar et al. (2023) [27]	hydrogen flow and pressures over time	-	-	System level
Onorato et al. (2022) [28]	<ul style="list-style-type: none"> • pressure profile in time • comparison of different layouts 	-	yes	Aircraft level
Alsamri et al. (2023) [29]	impact of hydrogen propulsion on emissions, cost, and performance	-	yes	Aircraft level

Table 2.2: Literature review overview table - Tank structure

Ref.	Tank Structure								
	Model Scope			Type	Shape	Pressure			Materials
	Geometrical	Mechanical	Thermal			Liquid Level	Pressure Fluctuations	Pressures Considered	
Verstraete (2009) [19]	-	Eq. (ASME)	Eq.	integral	cylindrical	97%	yes	P _{op} : 1.2 bar	Al 2219
Verstraete et al. (2010) [20]	-	Eq.	Eq.	integral	cylindrical	97%	yes	P _{fill} : 1.2 bar P _{vent} : 3.5 bar	Al alloy
Winnefeld et al. (2018) [21]	Eq.	Eq.	Eq.	non-integral	elliptical (parametric model)	97%	yes	P _{fill} : 1.2 bar P _{vent} : 1.448 bar	Al 2219
Mantzaroudis and Theotokoglou (2023) [22]	Eq.	von Mises stress analysis	PD	non-integral	parametric model (from Winnefeld et al.)	93%	-	P: 170 kPa	Al 2219
Palladino et al. (2021) [23]	Eq.	Eq.	Eq.	-	parametric model (from Winnefeld et al.) cylindrical tanks modelled for the study	-	-	-	Al 2219
Colozza et al. (2002) [24]	Eq.	Eq.	Eq.	-	cylindrical with hemispherical caps, and spherical	92.8%	-	P: 21 psi	-
Gomez and Smith (2019) [25]	-	PD	Eq.	integral	cylindrical with semi-spherical caps	94.8%	yes	P _{vent} : 25psi	Al 2219 (Al 7075 for structure, Ti-Al alloy for stiffeners)
Shank et al. (2023) [26]	PD	PD	Eq.	-	cylindrical with hemispherical caps, and spherical	100%	-	-	Al
Sarkar et al. (2023) [27]	-	PD	Eq.	-	cylindrical	94%	-	P: 21 psi	Al 2219, Al 2024
Onorato et al. (2022) [28]	-	Eq.	Eq.	integral and non-integral	cylindrical with caps	95.4%	yes	P _{fill} : 125 kPa P _{vent} : 250 kPa	Al 2014
Alsamri et al. (2023) [29]	Eq.	Eq.	Eq.	-	cylindrical with hemispherical caps	92.8%	-	-	Al 2014

Eq.: equations
PD: pre-defined

Table 2.3: Literature review overview table - Insulation

Ref.	Insulation				
	Model Scope	Config.	Temperature	Exposure Time	Materials
Verstraete (2009) [19]	<ul style="list-style-type: none"> • internal heat convection • heat conduction through insulation • external heat convection 	external	ΔT : 250-300 °C	-	foam (polyurethane, Rohacell) MLI
Verstraete et al. (2010) [20]	<ul style="list-style-type: none"> • internal heat convection • heat conduction through insulation • external heat convection • external heat radiation 	external	-	hold time: 2h	foam MLI
Winnefeld et al. (2018) [21]	<ul style="list-style-type: none"> • internal heat convection • heat conduction through tank wall • heat conduction through insulation • external heat convection • external heat radiation 	external	ΔT : 300 K	hold time: 2h	Rohacell foam
Palladino et al. (2021) [23]	<ul style="list-style-type: none"> • internal heat convection • heat conduction through tank wall • heat conduction through insulation • external heat convection 	external	-	-	Rohacell foam
Mantzaroudis and Theotokoglou (2023) [22]	<ul style="list-style-type: none"> • internal heat convection • heat conduction through tank wall • heat conduction through insulation • external heat convection • external heat radiation 	external	T_{in} : 20 K T_{out} : 283 K	-	polyurethane foam
Colozza et al. (2002) [24]	<ul style="list-style-type: none"> • heat conduction through insulation • external heat convection • external heat radiation 	external	T_{in} : 13 K	storage duration: 8h	foams: polymethacrylimide, polyurethane, polyvinylchloride, chopped glass fiber MLI with vacuum: Evacuated aluminum foil with fluffy glass mats Evacuated aluminum foil and glass paper laminate Evacuated silica powder
Gomez and Smith (2019) [25]	<ul style="list-style-type: none"> • heat conduction through insulation • external heat convection • external heat radiation 	internal	T_{in} : 22.5 K T_{out} : 281.9 K	-	polyurethane
Shank et al. (2023) [26]	<ul style="list-style-type: none"> • internal heat convection • heat conduction through tank wall • heat conduction through insulation • external heat convection • external heat radiation 	external	T_{in} : 28.7 K T_{out} : 218.9 K (in-flight) T_{out} : 322 K (on-ground)	-	foams: Expanded Polystyrene (EPS) Glass bubbles insulation MLI without vacuum: layers of EPS and coated Myler

Continued on the next page

Ref.	Insulation				
	Model Scope	Config.	Temperature	Exposure Time	Materials
Sarkar et al. (2023) [27]	<ul style="list-style-type: none"> internal heat convection heat transfer through tank wall 	external	T_{in} : 84 K T_{out} : 222 K (in-flight) T_{out} : 290 K (on-ground)	8h	polyurethane
Onorato et al. (2022) [28]	<ul style="list-style-type: none"> conduction through insulation 	external	T_{in} : 20 K T_{out} : 296 K (integral tank) T_{out} : ISA + 24.5 K (non-integral tank)	-	polyurethane
Alsamri et al. (2023) [29]	<ul style="list-style-type: none"> heat transfer through tank insulation 	external	T_{out} : 288.15 K	-	MLI

Chapter 3

Methodology

This chapter describes the methodology used in the development of the here-presented hydrogen tank sizing model, addressing the gaps identified in the literature in Section 2.3. An overview of the methodology is presented first, followed by a more detailed description of each of its main steps.

3.1 Methodology Overview

The objective of the developed model is to size the hydrogen tank based on the amount of hydrogen to be stored in it. Ultimately, this would lead to the exploration and definition of the storage tanks' placement layout in the aircraft. The energy required to complete the aircraft's mission is the starting point of the model. The methodology (shown in figure 3.1) is based on three main steps:

- (1) calculation of the required hydrogen volume
- (2) definition of the internal tank geometry
- (3) definition of the external tank geometry

Depending on the installation constraints, steps 2 and 3 might need to be iterated.

First, the properties of the hydrogen, such as its mass, density and pressure, are used to determine the volume of hydrogen that would need to be stored in the tank. Then, to size the internal geometry of the tank, geometrical parameters of the tank are used in addition to the determined volume, as well as tank filling considerations. Finally, the external geometry and mass of the tank depend on the insulation chosen to maintain the hydrogen at cryogenic temperatures. Knowing the aircraft geometry and some installation constraints, an exploration of the tank layout in the aircraft is done.

3.2 Required Hydrogen Volume

The main variable determining the volume of hydrogen is the mass of hydrogen to be stored, which can be either a direct user input or can be determined using the energy required for a certain mission and the specific energy of hydrogen. However, some additional considerations also contribute to the definition of the tank volume and will be explained in the following subsections.

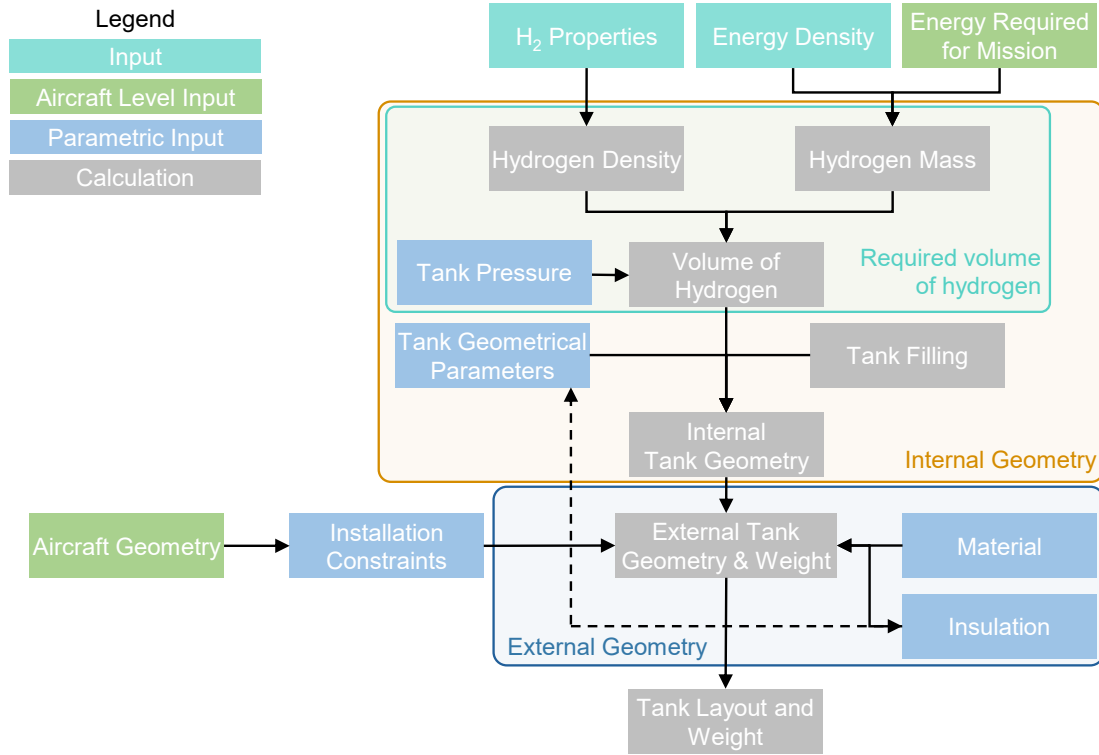


Figure 3.1: Methodology overview

3.2.1 Hydrogen Properties

The pressure rise inside a tank filled at 100% with saturated liquid is higher than in a tank filled with a two-phase mixture. To avoid overpressure, a two-phase mixture is preferred, as the presence of the gas phase at all times allows for rapid venting and, therefore, pressure regulation. Additionally, a smaller mass of hydrogen needs to be removed when gaseous hydrogen instead of liquid hydrogen is vented [19]. Thus, the tank is considered to contain hydrogen in liquid and gaseous phases, where these phases are in thermodynamic equilibrium. The thermodynamic properties of hydrogen at saturated state are taken from hydrogen properties data sheets [30]. Each temperature has a corresponding pressure, as well as a density value for the liquid and the gaseous portion of the mixture. A plot of the density vs. pressure for fully liquid and fully gaseous hydrogen can be built as in figure 3.2. The plot allows to observe the variation in density of liquid and gaseous hydrogen at different pressures. While on ground or during the aircraft mission, the pressure in the tank can increase. Venting is hence necessary once the pressure inside the tank reaches the maximum allowable tank pressure, denoted as P_{vent} .

A certain gaseous volume fraction has to be present in the tank to allow venting as if liquid hydrogen is vented; a higher mass of vented hydrogen is necessary to attain sufficient pressure drop rates [21]. The relationship between the volume of liquid and the total volume of hydrogen in the tank is defined as follows:

$$y = \frac{V_{liquid}}{V_{total}} \quad (1)$$

The rest of the volume is considered to be gaseous hydrogen.

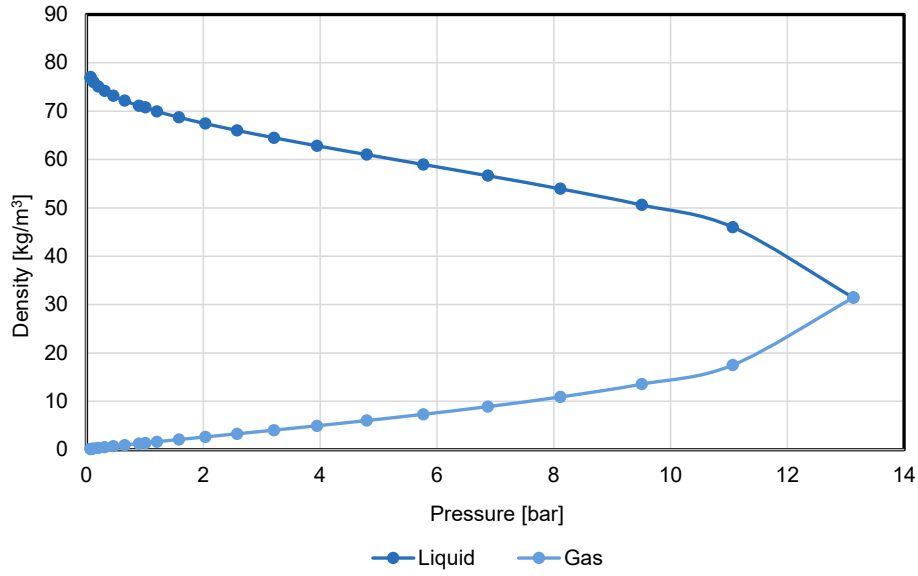


Figure 3.2: Density as a function of pressure of hydrogen gas and liquid

As the tank contains a mixture, the mean overall density is considered, and the composition of the mixture is to be taken into account. Figure 3.3 shows a nominal P - ν curve as well as some parameters used in the derivation of the equation used to calculate the average hydrogen density of the mixture. The states of the substance involving a mixture of gaseous and liquid phases in equilibrium lie in the region under the curve [31]. ν_f denotes the specific volume of the liquid state, ν_g denotes the specific volume of the gaseous state. ν_{fg} refers to the specific volume difference between the saturated gas and the saturated liquid.

To examine the mixture and its properties, it is necessary to know the proportion of liquid and gaseous phases in it. The quality, x , or in other words, the ratio of the mass of saturated vapour to the total mass of the mixture, defines this proportion [31]. The quality can, therefore, take values between 0 and 1, where saturated liquid has a quality of 0 while saturated vapour has a quality of 1. As a saturated mixture can be considered a combination of saturated liquid and saturated gas, the properties of the mixture can be defined as the average properties of the saturated liquid-vapour phase [31]. ν_{avg} is, thus, the average specific volume of the gas and liquid in the mixture. The average specific volume is denoted as:

$$\nu_{avg} = \nu_f + x \nu_{fg} \quad (2)$$

where x is the ratio of the mass of saturated vapour to the total mass of the mixture.

$$x = \frac{m_{vapor}}{m_{total}} = \frac{m_g}{m_f + m_g} \quad (3)$$

Equation (4) results from equation (2). The derivation of the equation to determine the average density of the liquid-gas mixture based on the quality in the tank is given in appendix A.1.

$$\rho_{avg} = \frac{\rho_g \rho_f}{\rho_g + x \rho_f - x \rho_g} \quad (4)$$

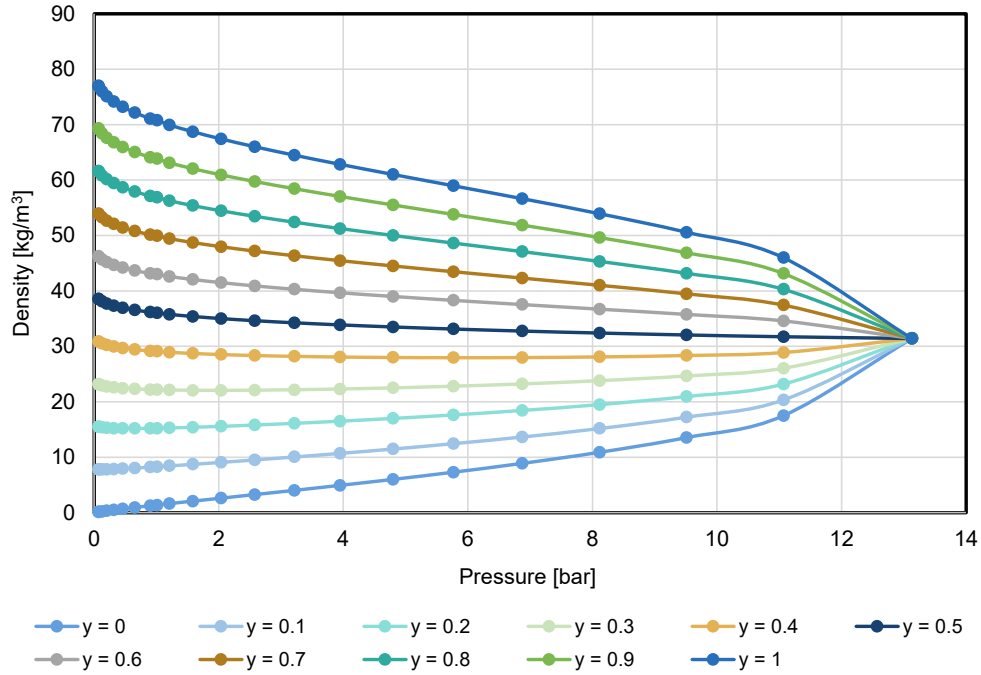


Figure 3.4: Average density of hydrogen at various volume fractions

3.2.2 Tank Filling Level

In case of boil-off, a certain amount of gas has to be available for venting, as described in section 3.2.1. If a certain percentage of the total volume is desired as allowance at the maximum pressure of the tank (at venting pressure P_{vent}), the ratio of liquid to the total volume at filling pressure needs to be determined. This is because, at lower pressure, the density of gas would be lower and, therefore, for a constant mass, would take more volume.

If the density of the substances at venting pressure serves as a reference, at an arbitrary lower pressure, the liquid density would be lower, and its volume would be higher. Inversely, at venting pressure, the gas density would be higher and its volume lower than at a lower pressure. Being aware of these variations of density and volume, the aim is then to determine the level to which the tank can be filled at a lower pressure (P_{fill}) while maintaining a certain desired allowance at the maximum pressure.

According to Verstraete [19], in case of degradation of the insulation of the tank, the pressure would increase so quickly that no fuel can be withdrawn. As the mean density of hydrogen does not change during the process, the fill level of the tank is determined with respect to the filling and venting pressures. To carry the calculations determining the level at which the tank has to be filled at filling pressure, a constant density of the two-phase mixture between the fill and the venting pressure is assumed ($\rho(P_{fill}) = \rho(P_{vent}) = constant$). The main steps to determine the fill level are the following:

- (1) Selecting a venting pressure and a maximum liquid hydrogen percentage at the maximum (venting) pressure, then finding the corresponding average density
- (2) Setting the calculated average density to be the density considered at all pressures

- (3) Selecting the filling pressure, and at that filling pressure and previously found average density, determining the level up to which the tank can be filled at filling pressure

Figure 3.5 serves to illustrate this procedure and shows an example of the relation of density and pressure for different liquid volume fractions. At a given venting pressure (3.5 bar), taking as an example the values provided by [19] and presented in table 2.2, and a selected venting allowance (here 3% of gaseous hydrogen and therefore 97% liquid), the average density of the mixture can be determined (ρ_{avg}). To have a tank filled at 97% at the maximum pressure and keeping the average density on the tank constant, at the filling pressure (selected here to be around 1.2 bar), the tank would need to be filled at a lower percentage (in this example, at 88%).

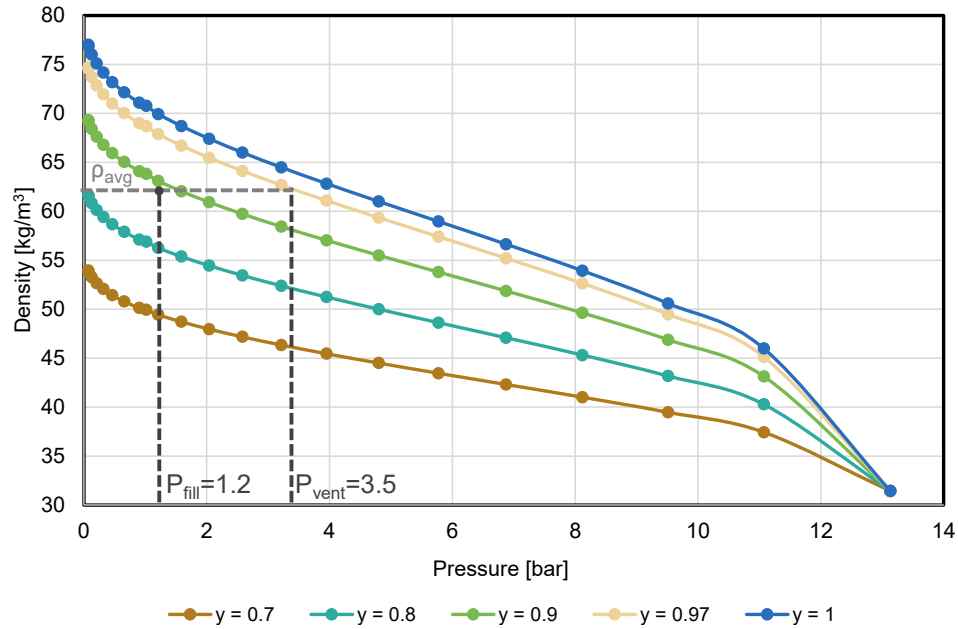


Figure 3.5: Relationship between the average density and the filling and venting pressures

The level at which the tank needs to be filled at filling pressure to be able to accommodate the desired allowance at venting pressure is described by equation (7) and it is derived from equation (6). Appendix A.1 shows the full derivation.

$$y = \frac{\rho_g - \rho_{avg}}{\rho_g - \rho_f} \quad (7)$$

The average density of the mixture was previously found with equation (6). The densities of gas and liquid are the ones at filling pressure determined from hydrogen properties data [30]. The filling level (at filling pressure) can thus be obtained with equation (7).

In summary, venting pressure and the ratio of liquid in the tank at venting pressure are used to find the average density of the mixture. That average density of the mixture, along with the desired filling pressure, is used to find the level at which the tank has to be filled at filling pressure. Figure 3.6 shows a plot of the density of the mixture as a function of the filling pressure, for different venting pressures. Building on the previous example, figure 3.7 shows the filling level of a tank (88%) with a venting pressure of 3.5 bars and a filling pressure of 1.2 bars.

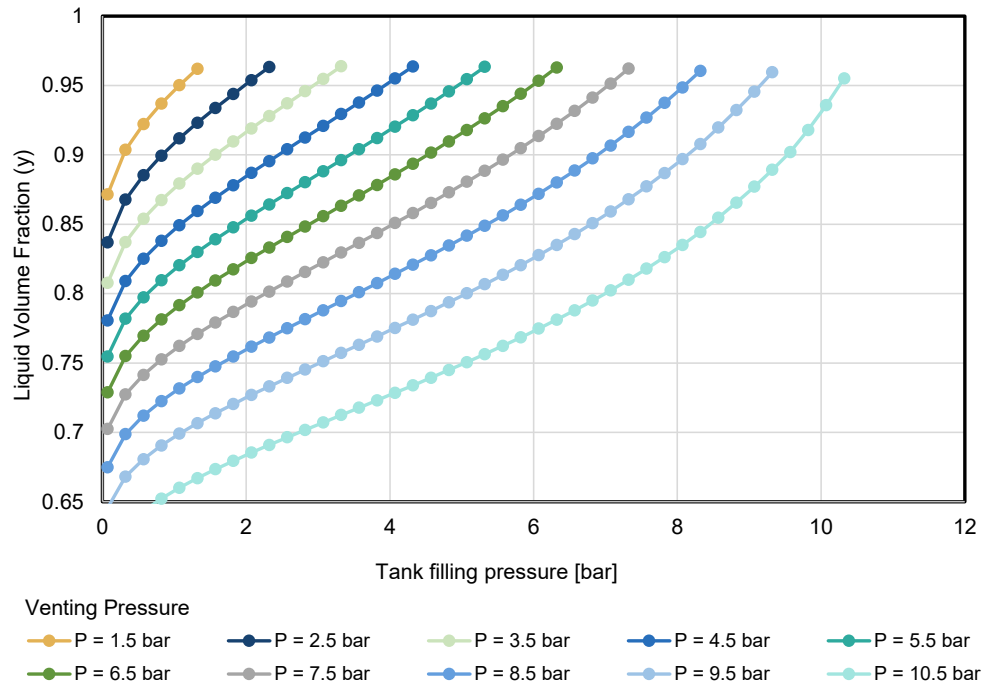


Figure 3.6: Liquid volume fraction with respect to various fill and venting pressures

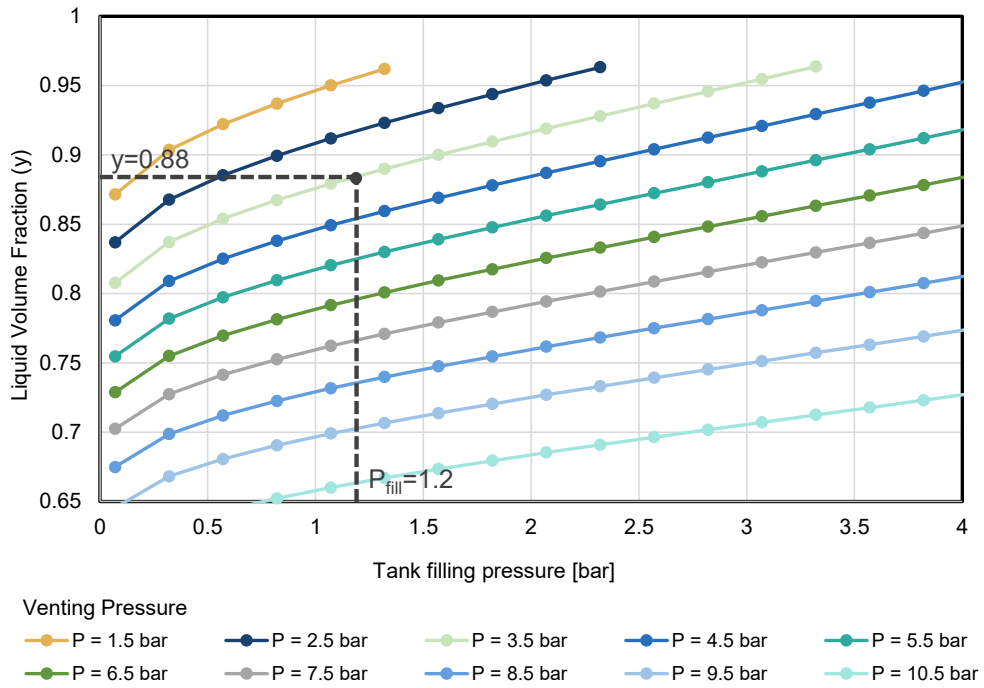


Figure 3.7: Liquid volume fraction for given venting and filling pressures

Knowing the density and the mass of hydrogen needed for the aircraft mission, the volume of liquid hydrogen is determined. The fill level of the tank is then used to determine the total volume of the tank using equation (1).

3.3 Internal Tank Geometry Sizing

The definition of the internal tank geometry starts with the volume of hydrogen to be stored, along with the tank capacity, leading to the establishment of the dimensions and the shape of the tank. Once the tank shape has been determined, the mass of the tank can be calculated according to the selected material for the tank walls.

The tank's geometry is assumed to be composed of an elliptical cylinder shell and two ellipsoidal heads at each end, as described by Winnefeld et al. [21]. The geometrical parameters defining the shape of the tank are presented in Figure 3.8a, while 3.8b shows a notional 3D representation of such a tank.

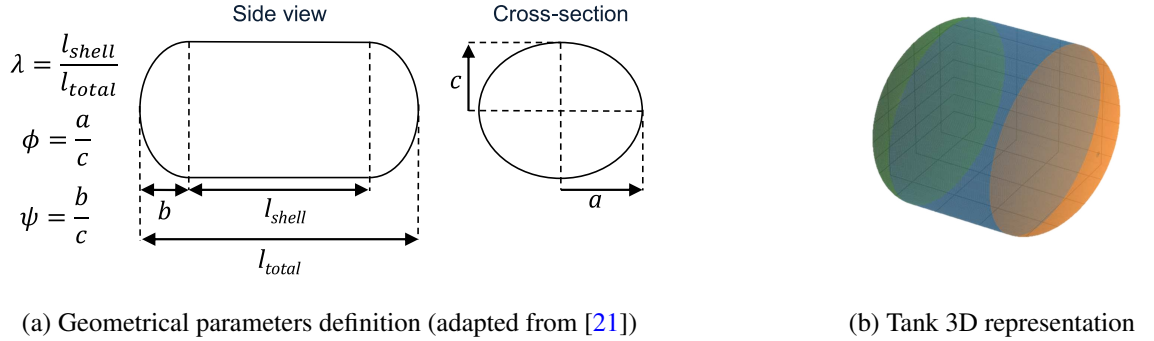


Figure 3.8: Geometrical representation of a modelled tank

The parameter ϕ is the ratio between the ellipsoidal axes; it describes how round the tank is, ψ describes the shape of the tank heads or how protruded they are, and λ represents the ratio of the length of the shell vs. the total length of the tank. For $\lambda = 0$, the tank would not have a shell, but only heads, inversely with λ approaching 1, the shell length would tend to infinity. With $\lambda = 1$, the model becomes under-constraint as b and therefore ϕ would be equal to 0.

Table 3.1 shows a summary of the geometrical ratios, and their definitions and boundaries.

Table 3.1: Definition of tank geometrical parameters

Ratio	Definition	Bounds
ϕ	How round the tank is	$0 < \phi < \infty$
ψ	How (round and) protruded the tank heads are	$0 < \psi < \infty$
λ	How much of the tank is heads or shell (ratio between the shell and overall length)	$0 \leq \lambda < 1$

The tank being composed of an elliptical shell and two ellipsoidal heads at each end, the following equations defining the geometry of the tank can be derived (note that here l_{shell} is defined as l_s and l_{total} is defined as l_t for simplicity):

$$a = \left(\frac{3V_t \phi^2 (1 - \lambda)}{\pi \phi (2\lambda + 4)} \right)^{1/3} \quad (8)$$

$$b = \psi c \quad (9)$$

$$c = \frac{a}{\phi} \quad (10)$$

$$l_s = \frac{V_t - \frac{4}{3}\pi abc}{\pi ac} \quad (11)$$

$$l_t = l_s - 2b \quad (12)$$

$$V_t = \pi a c l_s + \frac{4}{3}\pi abc \quad (13)$$

As shown in figure 3.8b, the parameters defining the tank are $a, b, c, l_s, l_t, \phi, \psi, \lambda, V_t$. Using equations (8) to (13), when four of these parameters are defined, the others can be calculated and the shape of the tank defined.

The ratios ϕ, ψ and λ define how round and protruded the shell or the heads of the tank are. Figure 3.9 presents examples of tanks where one of these parameters is varied and the other two are kept constant for a certain fixed volume to illustrate the effect of each of these parameters on the shape of the tank. In summary, these three dimensionless parameters enable a flexible tank design that can adapt to predefined geometric constraints, such as a pre-defined constant volume.

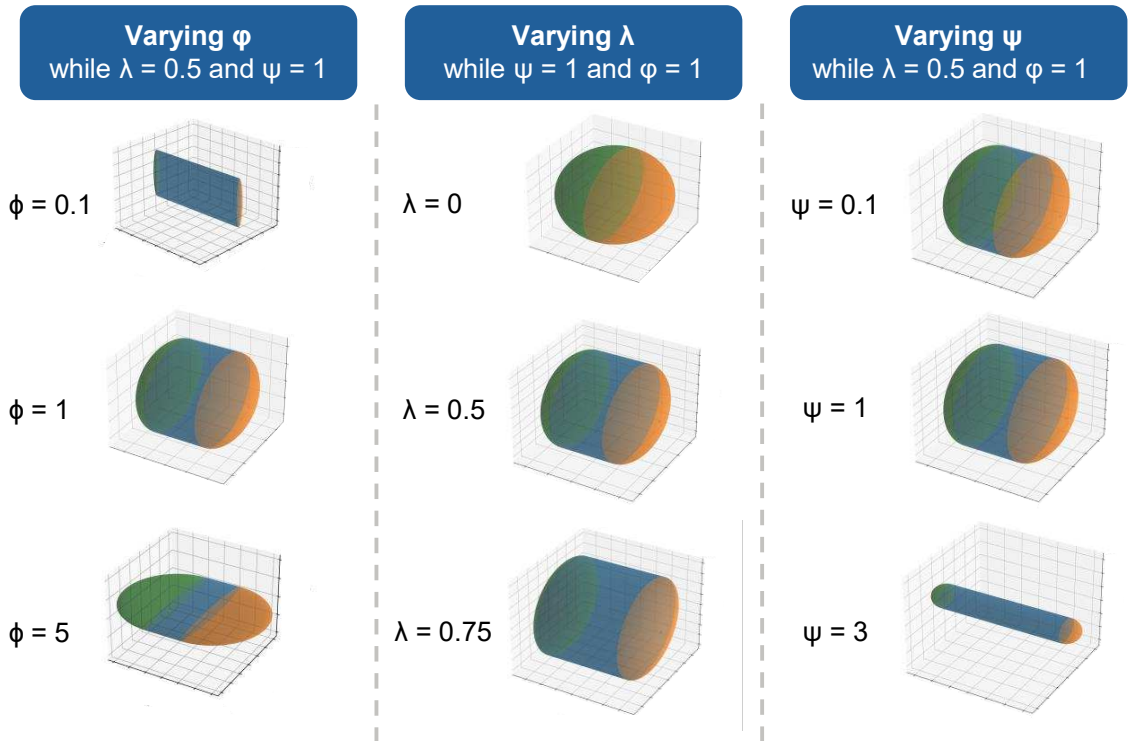


Figure 3.9: Variation of tank shape with varying geometrical parameters

Once the parameters defining the tank shape are determined, the surface area of the tank is calculated. This is crucial for the calculation of the tank mass, as well as for the insulation module of the tool, which will be covered in section 3.4. Equation (14) adapted from [32], [33] is used to calculate the surface area of the tank, where the first part refers to the elliptical cylinder, or shell of the tank and the second part of the equation refers to the semi-ellipsoidal caps of the tank.

$$A = \left(\int_0^{2\pi} \sqrt{a^2 \sin^2(\theta) + c^2 \cos^2(\theta)} d\theta \right) l_s + 2 \cdot 2\pi \left(\frac{(ab)^{1.6075} + (bc)^{1.6075} + (ac)^{1.6075}}{3} \right)^{\frac{1}{1.6075}} \quad (14)$$

Another important parameter in the calculation of the tank mass is the thickness of the tank walls. This is determined based on the internal pressure the tank is designed to withstand using equation (15) [21] and the material properties of the tank wall.

$$K \geq P \left[\frac{a+c}{2s_w} \left(1 + 2 \left(1 + 3.6 \frac{P}{E_Y} \left(\frac{a+c}{2s_w} \right)^3 \right) \left(\frac{a-c}{a+c} \right) \right) + \frac{1}{2} \right] \quad (15)$$

Where K is the limiting stress of the tank, P is the maximum pressure inside the tank, E_Y is Young's modulus, and s_w is the wall thickness of the tank.

The model is parametrized allowing users to adjust various inputs, including material properties, to explore different scenarios. Using the density of the chosen material, the calculated surface area of the tank and the thickness of the wall, the mass of the tank can be calculated, leading to the completion of the internal geometry tank sizing.

3.4 External Tank Geometry Sizing

Because the hydrogen is kept in a liquid state inside the tank, the tank material and insulation required to sustain cryogenic temperatures are an integral part of the modelling process, impacting both the external geometry and the overall weight of the tank. Various insulation materials are investigated, looking at their thermal performance and weight. The insulation is then sized, ensuring that the selected material effectively maintains the desired cryogenic temperatures.

3.4.1 Insulation Materials

Three primary insulation categories are commonly referenced for cryogenic applications: foams, aerogels, and MLI. Some of these materials can be used with or without a vacuum layer. Table 3.2 outlines some key attributes of these insulation types.

Table 3.2: Insulation types characteristics overview (adapted from [34], [35])

Foams	Multi-layer insulation	Aerogels
<ul style="list-style-type: none"> • Well established • Low density, lightweight • Relatively high thermal conductivity (14-33 mW/mK) 	<ul style="list-style-type: none"> • Well established • Low thermal conductivity (2-24 mW/mK) 	<ul style="list-style-type: none"> • Newer technology • Limited mechanical properties • Low thermal conductivity (0.6-12 mW/mK)

The main parameters used to compare insulation materials are thermal conductivity and material density. A low thermal conductivity leads to thinner insulation, while a low density results in lower

mass. An ideal material would, therefore, have low thermal conductivity and density. However, as shown in the benchmark materials in figure 3.10, none of the insulation types has both advantages; a trade-off between the thickness (volume) and the mass of the different insulation is necessary.

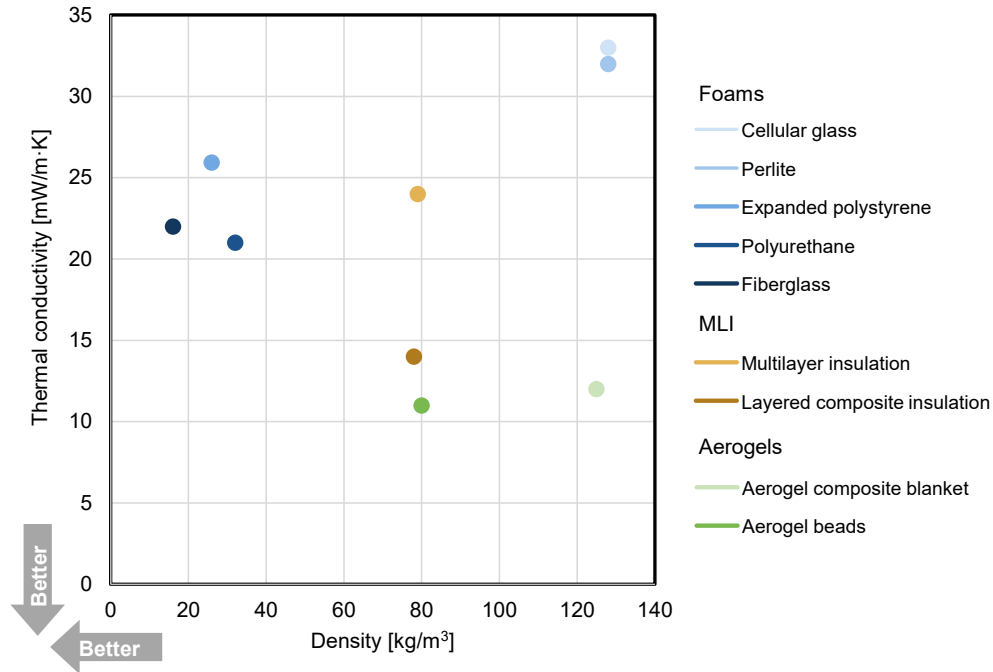


Figure 3.10: Insulation materials properties

Foams generally tend to have a lower density, which is advantageous but exhibit higher thermal conductivity, which is undesirable. In contrast, aerogels have a low thermal conductivity but a higher density. MLI tend to fall in the middle range for both conductivity and density compared to the other types of insulation.

Some of these materials can also be used in soft or hard vacuum environments to achieve even lower thermal conductivity. However, this setup requires a double-walled structure to maintain the vacuum [34], [35].

Figure 3.11 displays the properties of various insulation materials at different vacuum levels, detailed in appendix B. The thermal conductivity decreases in soft vacuum conditions and further decreases in hard vacuum. This reduction in thermal conductivity allows for thinner and, therefore, lighter insulation; however, as previously mentioned, a double-walled structure is required to maintain the vacuum, which can, in turn, add significant weight. A model needs to be developed to evaluate the trade-offs between the two insulation approaches and to analyze their performance. Figure 3.12 provides an overview of the structure of the insulation categories. The details of how these are modelled will be provided in section 3.4.2.

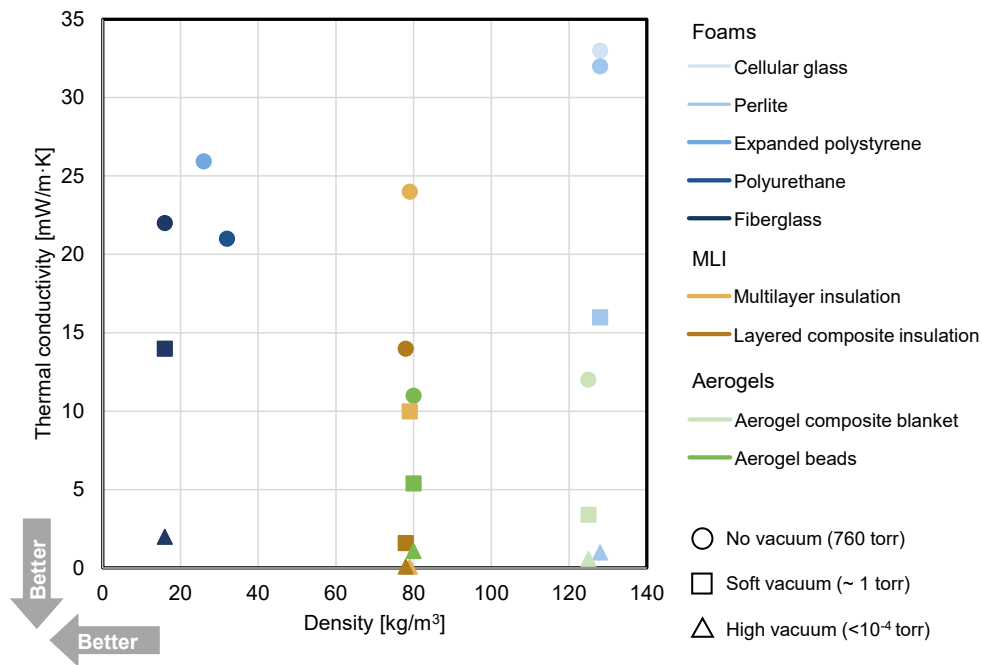


Figure 3.11: Insulation materials properties in vacuum

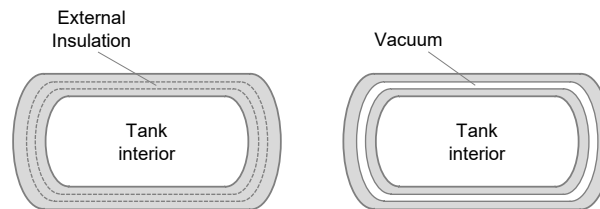


Figure 3.12: Overview of different insulation types

3.4.2 Insulation Sizing

The heat from the environment entering the liquid hydrogen tank causes the liquid to boil. The gas resulting from the boil-off process has to be vented to maintain the tank pressure and is, thus, lost to the environment. Effective insulation is required to minimize these losses. To size the tank's insulation, the thermal module of the tool accounts for the heat entering the tank over a certain time. The internal and external temperatures of the tank are key parameters in the insulation sizing. The thermal resistance and, consequently, the insulation thickness are calculated using one-dimensional heat transfer principles while taking into account the tank's geometry.

To minimize the boil-off and the subsequent loss of hydrogen, it is essential to calculate the amount of heat leading to the boil-off that passes through the insulation. The heat across the hydrogen storage tank is the energy raising the temperature from the filling temperature to the venting temperature and is calculated with equation (16)[31].

$$Q = m_{H_2} \cdot C_v \cdot (T_{vent} - T_{fill}) \quad (16)$$

Q is the heat transferred, m_{H_2} is the mass of hydrogen, C_v is the specific heat of hydrogen, T_{vent} is the temperature of hydrogen at venting pressure, and T_{fill} is the temperature of hydrogen at filling pressure.

The time t during which the tank is exposed to the environment and thus susceptible to heat transfer is also factored into the calculation to evaluate the total heat transfer over the exposure period. This exposure time is considered to be the time before boil-off begins to occur. The rate of heat transfer is calculated by:

$$\dot{Q} = \frac{Q}{t} \quad (17)$$

To determine the total resistance necessary to impede the heat transfer through the tank walls and the insulation, equation (18) is derived from the temperature difference between the external environment T_{env} and the tank interior T_{fill} , as well as the rate of heat transfer [31].

$$R_{total} = \frac{T_{env} - T_{fill}}{\dot{Q}} \quad (18)$$

Once the total thermal resistance required is determined, it can be achieved either through external insulation or vacuum-based insulation. The schematic representations of each approach are shown in figure 3.13 and will be discussed in detail in the following subsections.

External Insulation Sizing

As described by equation (18), the total thermal resistance depends on the temperature difference between the interior and the exterior of the tank and the heat transferred through the tank wall and insulation. This overall resistance consists of several parts: the resistance of the tank wall, of the insulation and of the surrounding air outside the tank.

The schematic in Figure 3.13a describes the model of external insulation in several layers inspired by [21]. In this configuration, the tank wall is covered by multiple layers of insulation and is exposed to the surrounding environment. Each of these components has associated thermal resistances. These resistances are outlined in equations (19) to (21) [36]: equation (19) defines the thermal resistance for conduction, equation (20) the thermal resistance for convection, and equation (21) the thermal resistance for radiation.

$$R_{conduction} = \frac{L}{k \cdot A} \quad (19)$$

where L is the characteristic length (in this case, the thickness of the layer), k is the thermal conductivity (in W/m · K), and A is the area (in m²).

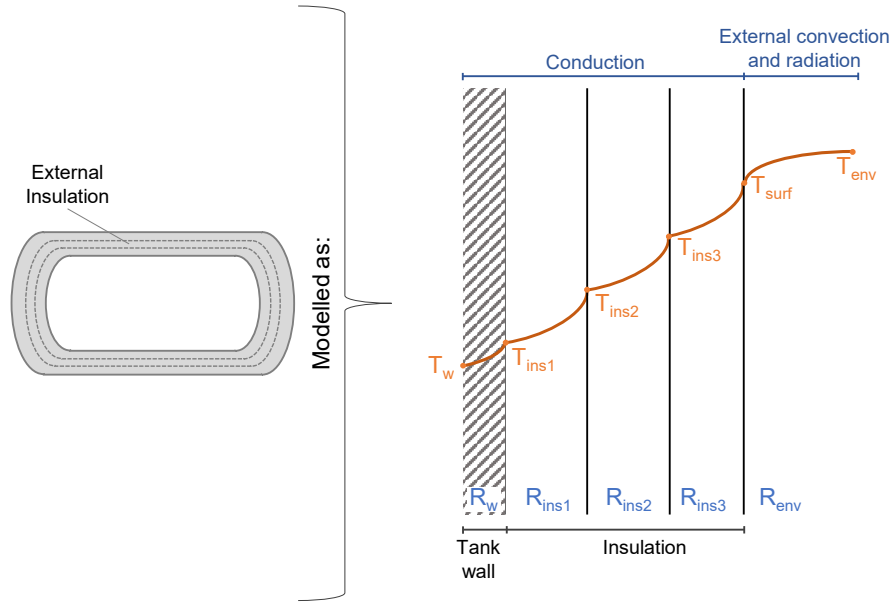
$$R_{convection} = \frac{1}{h \cdot A} \quad (20)$$

where h is the convection heat transfer coefficient (in W/m² · K).

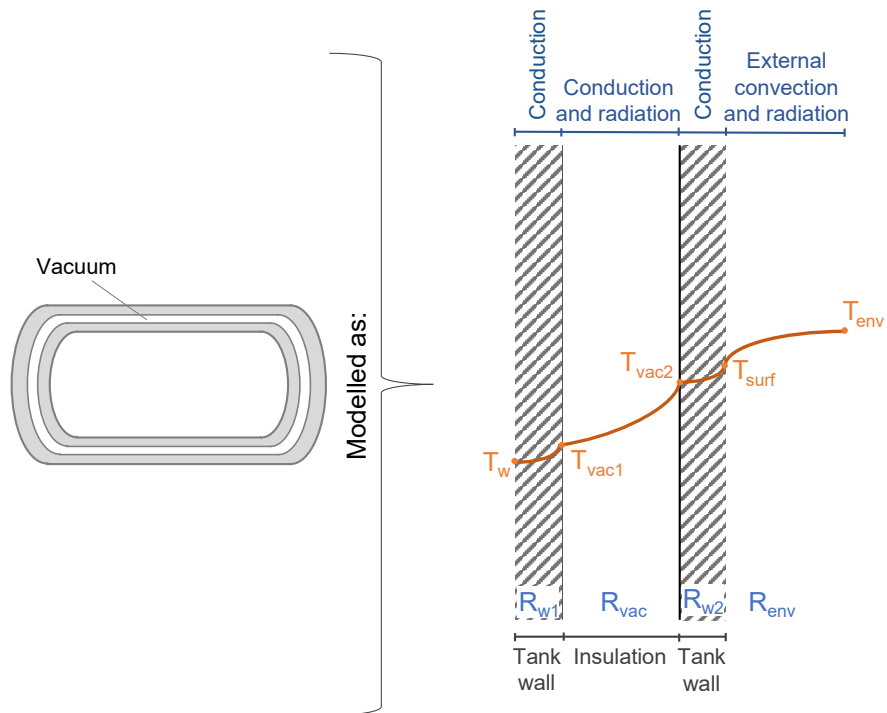
The equations leading to the definition of this coefficient are shown in appendix A.2.

$$R_{radiation} = \frac{1}{\varepsilon \cdot \sigma \cdot A \cdot (T_{env}^2 + T_{surf}^2) \cdot (T_{env} + T_{surf})} \quad (21)$$

where ε is the emissivity of the material, σ is the Stefan-Boltzmann constant ($5.67 \times 10^{-8} \text{ W/m}^2 \cdot \text{K}^4$) and T are the temperatures in the outside environment and at the surface.



(a) Modelling of external insulation



(b) Modelling of vacuum-based insulation

Figure 3.13: Schematic of different insulation types models

To mathematically represent the insulation of the tank and its thermal resistance, equation (18) is rearranged as:

$$\Delta T = R \cdot \dot{Q} \quad (22)$$

Building on this expression, the schematic in figure 3.13a is represented by the following system of equations:

$$\begin{pmatrix} -1 & 1 & 0 & 0 & 0 & 0 \\ 0 & -1 & 1 & 0 & 0 & 0 \\ 0 & 0 & -1 & 1 & 0 & 0 \\ 0 & 0 & 0 & -1 & 1 & 0 \\ 0 & 0 & 0 & 0 & -1 & 1 \end{pmatrix} \begin{pmatrix} T_w \\ T_{ins1} \\ T_{ins2} \\ T_{ins3} \\ T_{surf} \\ T_{env} \end{pmatrix} = \begin{pmatrix} R_w \\ R_{ins1} \\ R_{ins2} \\ R_{ins3} \\ R_{env} \end{pmatrix} \dot{Q} \quad (23)$$

As mentioned previously, the resistance of each layer has associated heat transfer mechanisms: the tank wall and the insulation both provide conductive resistance (described by equation (19)), while the external environment introduces convective and radiative resistances (described by a combination of equations (20) and (21)). Each of these resistance terms is substituted into the system of equations accordingly, and the resulting system is solved for the unknown variables, leading to the definition of the insulation thickness.

Building on this, and similarly to the tank mass, the insulation mass is calculated using the thickness and material density of the insulation layer, leading to the completed sizing of the tank insulation.

Vacuum-based Insulation sizing

The methodology to size the vacuum-based insulation is similar to the one sizing the external insulation described in the previous section. However, here, the insulation used to provide the total resistance determined by equation (18) consists of the resistance of the internal wall of the tank, of a vacuumed layer of insulation, of another tank wall and finally of the surrounding air outside the tank. This insulation type is illustrated in figure 3.13b and is represented by the following system of equations:

$$\begin{pmatrix} -1 & 1 & 0 & 0 & 0 \\ 0 & -1 & 1 & 0 & 0 \\ 0 & 0 & -1 & 1 & 0 \\ 0 & 0 & 0 & -1 & 1 \end{pmatrix} \begin{pmatrix} T_w \\ T_{vac1} \\ T_{vac2} \\ T_{surf} \\ T_{env} \end{pmatrix} = \begin{pmatrix} R_{w1} \\ R_{vac} \\ R_{w2} \\ R_{env} \end{pmatrix} \dot{Q} \quad (24)$$

As for the external insulation, the vacuum-based insulation was assumed to have a resistance associated to each component of it. As illustrated in figure 3.13b, the two tank walls provide conductive resistance, the insulation layer is assumed to provide conductive and radiative resistance, and as for the external insulation, the external environment is associated with convective and radiative resistances. Equations (19) to (21) are substituted into the system of equations, which is then solved for the unknowns, such that the thickness of the vacuum-based insulation layer is determined. The insulation mass associated with that layer is calculated using that thickness, the surface area of the tank, and the density of the chosen insulation material.

3.5 Methodology Implementation

The hydrogen tank sizing methodology described in this section and illustrated in figure 3.1 is developed in a Python-based tool comprising three main modules: the hydrogen properties, the tank geometry, and the insulation as shown in figure 3.14. As illustrated, the main tool inputs are the tank pressures, the mass of hydrogen to be stored, some geometrical parameters and the exposure time to the environment. The tool solves for the undefined geometrical parameters, as well as the wall and insulation thickness and mass. Appendix C shows a snippet of the geometrical solver implemented in the tool, allowing to find the missing geometrical parameters. The implementation of the methodology in Python makes it flexible and allows for the exploration of different scenarios based on various inputs. It also enables a freer exploration of the design parameters and the overall impact on the tank configuration. Furthermore, the integration into a MDAO framework also puts requirements on the implementation of the methodology, as the tool has to adhere to a structure that allows smooth integration with other modules.

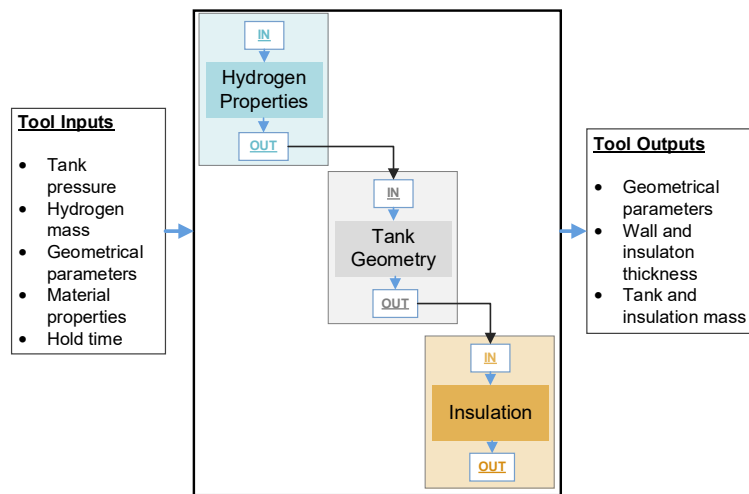


Figure 3.14: Tool code modules overview

The tank-sizing tool is developed to be integrated into a MDAO workflow, where it will interface with aircraft sizing and performance tools, and an alternative propulsion tool upstream, as well as a Life-Cycle Assessment (LCA) model downstream to evaluate the impact of the hydrogen-based propulsion on the aircraft-level. This integration is in the context of the broader EAP project aiming to explore advanced propulsion concepts, among which hydrogen-powered aircraft designs. As the development of other tools and the integration within the framework is ongoing and not yet ready for demonstration, the work focuses only on the hydrogen tank sizing module, providing the groundwork for future integration in the MDAO workflow.

3.6 Hydrogen Tank Sizing Tool Validation

To ensure the accuracy of the hydrogen tank sizing model and the correct functionality of the developed tool, it is necessary to validate the entire methodology by integrating all modules and testing them in a realistic real-life scenario.

Collected data from the storage tank industry was used in the validation process to provide realistic specifications of tank dimensions, pressure ratings, and material properties. Due to the lack of readily available data specific to hydrogen storage tanks for aerospace applications, the tool was validated using data from stationary cryogenic tanks [37]. Datasheets from manufacturers, while fairly complete, for stationary hydrogen storage, lack details for aerospace applications. This limits the opportunity to address and validate some aerospace-specific challenges, such as lighter structural weight and specific performance requirements.

The validation involved sizing tanks with known geometric parameters such as diameter and height, along with materials for the tank walls and insulation. The developed model was used to size the overall tank volume and mass based on these inputs. Appendix D outlines the materials and assumed properties used for the validation process. The validation set includes tanks of various storage volumes, which are sized for 1.8 MPa and 24h hold time. Figure 3.15 compares the computed mass of tanks of various sizes with the mass from industrial data. The results show that the tool predicted the mass of the smaller tanks in the set more accurately. For tanks up to 37 m³, corresponding to 900 kg of hydrogen, the error is below 15%. In the context of this research and the EAP project related to it, tanks of similar order of magnitude are considered. The test cases presented in chapter 4 focus on tanks with a volume of approximately 10 m³ and containing 345 kg of hydrogen.

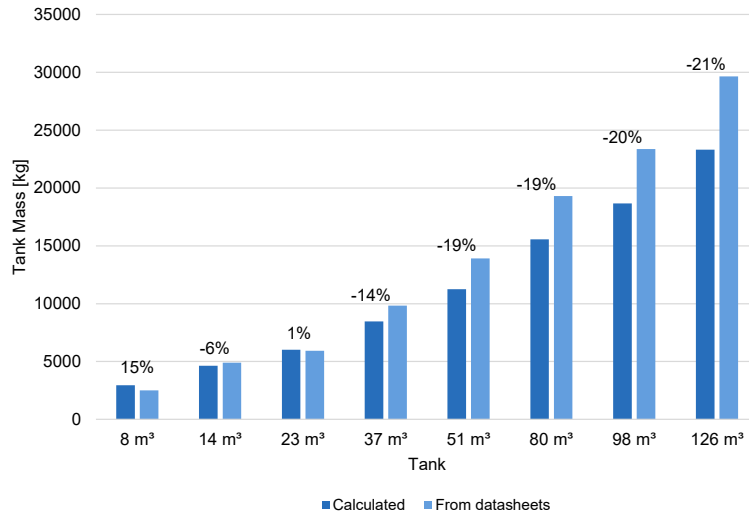


Figure 3.15: Comparison of calculated tank mass with data from industry

On the other hand, the larger tanks’ mass was consistently underpredicted by around 20%. This discrepancy can be attributed to the fact that the tool calculates only the mass of the tank structure and insulation, while the available data for stationary tanks used in the validation process includes the mass of additional components, such as supports and piping. Stationary tanks serve as a valuable starting point for validation data; however, their heavier structures and different operating conditions pose a validation challenge, highlighting the limitations of currently available data. Conversely, validating the tool using the available data for stationary tanks demonstrates the ability of the model to adapt to tanks of different applications, using various materials at different environmental conditions.

3.7 Summary of Chapter 3

In summary, the methodology used to size cryogenic tanks presented in this work is based on three main aspects: geometrical, mechanical, and thermal. The geometry of the tank is determined based on the required hydrogen volume for the aircraft mission, taking into account the physical properties of hydrogen and the conditions to which it is subjected. Following, the structure of the tank is sized as well as the insulation, based on selected insulation materials, tank exposure time and environmental conditions. This methodology is implemented in a Python-based tool, offering flexibility for the exploration of various test cases with diverse input parameters. The tool is validated using real-world cryogenic tank data, showcasing its ability to size tanks of various dimensions.

Chapter 4

Application Cases

The cryogenic tank sizing model presented in chapter 3 enables the exploration and evaluation of several sizing scenarios tailored to various applications. Each of the scenarios presented in figure 4.1 has different objectives and requires specific distinct inputs for the tank geometry definition described in section 3.3. This section focuses on presenting the capabilities of the tank sizing tool.

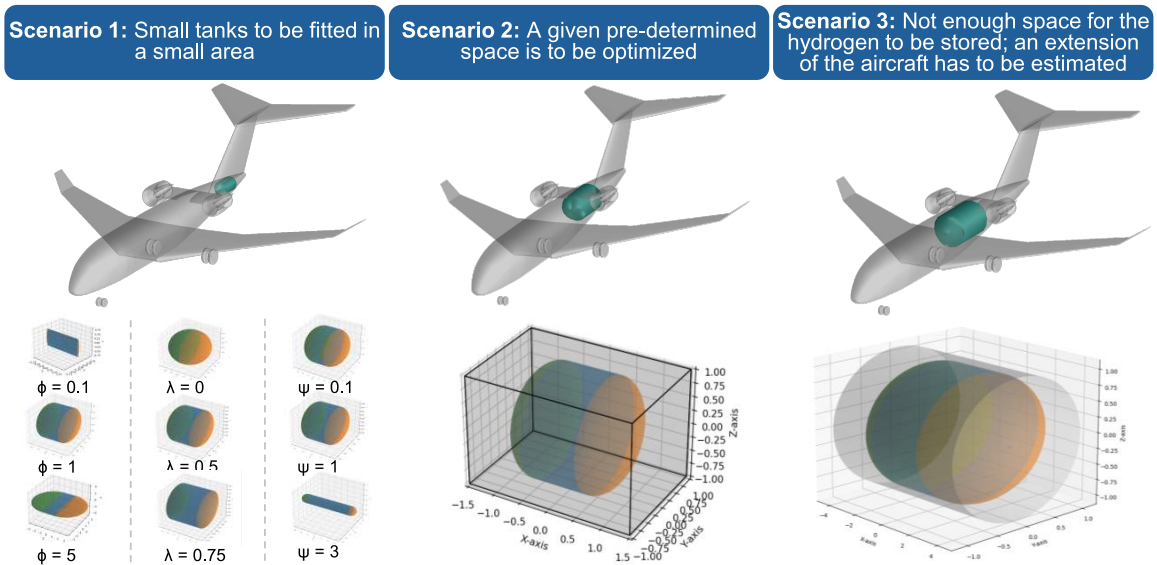


Figure 4.1: Tank sizing model application scenarios

Scenario 1 allows the exploration of various tank shapes based on the geometrical ratios introduced in section 3.3 (Figure 3.8). The geometrical ratios (ϕ , ψ , λ) are varied, allowing a flexible approach to exploring and designing more versatile tanks. This scenario is applicable, for example, when a small tank has to be fit within a small irregular space. This could be the case when replacing an **Auxiliary Power Unit (APU)** with a hydrogen-powered one or with a hydrogen fuel cell, and the tank is to be placed in the tail of the aircraft.

Scenario 2 considers a pre-defined allocated space for hydrogen storage. In this case, the tank has to store the necessary amount of hydrogen while fitting into a pre-determined space. If the hydrogen volume exceeds the pre-allocated volume, scenario 3 should be considered.

Scenario 3 applies when a large amount of hydrogen is to be stored, but there is insufficient space within the baseline aircraft structure and hence, an aircraft extension would be necessary. This scenario helps determine the length of the extension required to accommodate the volume of hydrogen to be stored.

The following sections showcase the tank sizing tool capabilities using different test cases.

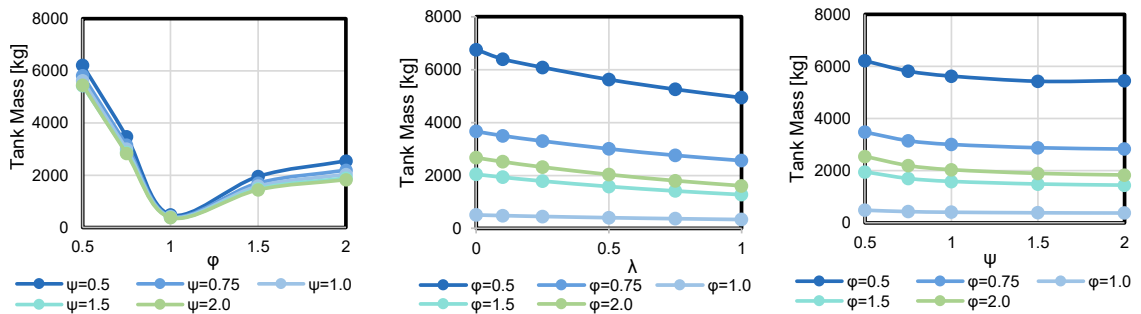
4.1 Variation of Tank Geometry

This application case, corresponding to scenario 1, offers insights into how tank mass varies with varying geometry. The geometrical ratios (described in figure 3.8a) are varied while keeping the volume of the tank constant, and the effect on the mass is assessed.

The assumptions used for this case study, such as the tank volume and wall properties, are listed in table 4.1. The values of ϕ and ψ were varied between 0.5 and 2, and the value of λ between 0 and 1; keeping one of the variables constant, the two other parameters were varied. Figure 4.2 illustrates the impact of varying the geometrical ratios ϕ , ψ , and λ on the tank mass. It is to be noted that only the mass of the internal tank is considered here; the insulation mass is not included.

Table 4.1: Assumptions in geometry variation study

Variable	Value
Hydrogen mass [kg]	345
Liquid level [%]	97
Tank volume [m ³]	11.3
Tank wall material	Al 2219
Material density [kg/m ³]	2840 [38]



(a) Impact of variation of ϕ on the tank mass (λ kept constant at 0.5) (b) Impact of variation of λ on the tank mass (ψ kept constant at 1) (c) Impact of variation of ψ on the tank mass (λ kept constant at 0.5)

Figure 4.2: Impact of geometrical ratios on the tank mass (excluding insulation)

As the value of ϕ deviates from 1, the tank's mass rapidly escalates to a range of values unrealistic for aerospace use; therefore, values near $\phi=1$ are truly meaningful, as the lowest weight is achieved with tanks with circular cross-sections. Figure 4.3 shows the impact of varying the geometrical ratios in the design space close to $\phi=1$. Studies on the volume occupied by these tanks are necessary to conduct trade-off analyses between mass savings and packing efficiency within a given space.

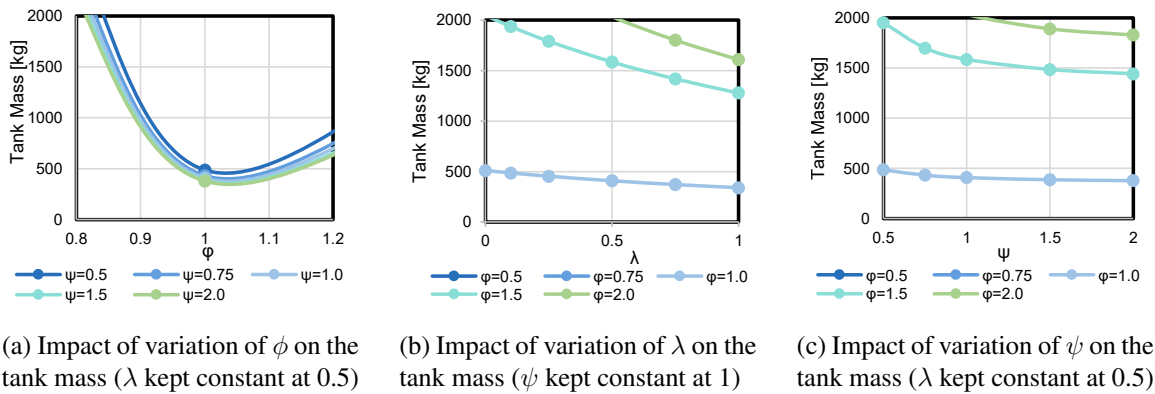
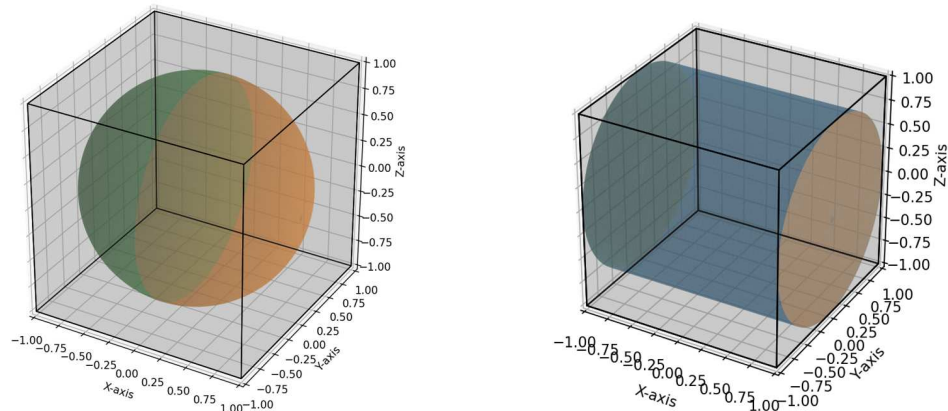


Figure 4.3: Impact of geometrical ratios on the tank mass (excluding insulation) - focus on $\phi = 1$

4.2 Tank Allocated Space

This application case is strongly related to the second scenario in which a pre-determined volume is to be optimized. Given a pre-allocated tank storage space, it is possible to investigate the ratio of the tank's volume to the available space - a key factor, as efficient use of space in an aircraft is of prime importance. The tool allows for trade-off studies between the volume occupied by the tank and its mass.

For a given space, a spherical tank would lead to the lowest mass, yet a spherical shape might not lead to the most efficient use of that space. Figure 4.4 portrays an allocated space (represented by a grey cubical box) in which tanks of different shapes but the same cross-sections are fitted. Figure 4.4a shows the most efficient shape in terms of mass (a sphere), while figure 4.4b pretenses the shape that maximizes space usage (a cylinder with flat ends). The former uses 52% of the available space, while the latter utilizes nearly 79%. The cylindrical tank, while being volumetrically more efficient, is about 50% heavier than the spherical tank. These are two contrasting examples of tanks within a cubical allocated space; however, similar studies can also be conducted on more versatile shapes.



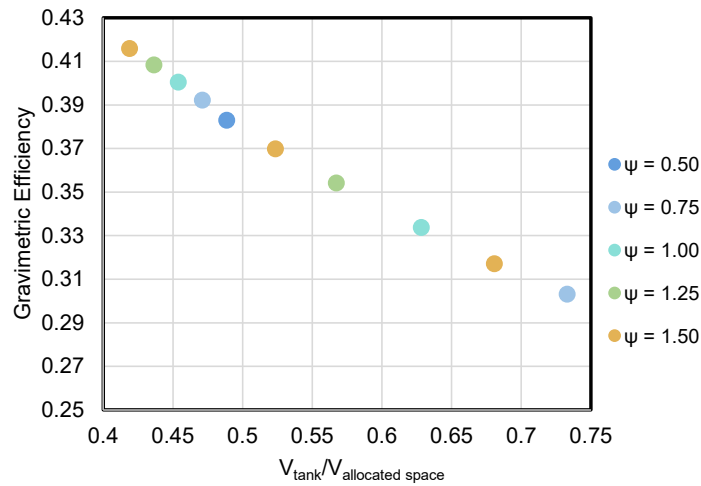
(a) Spherical tank in a pre-defined allocated volume

(b) Cylindrical tank in a pre-defined allocated volume

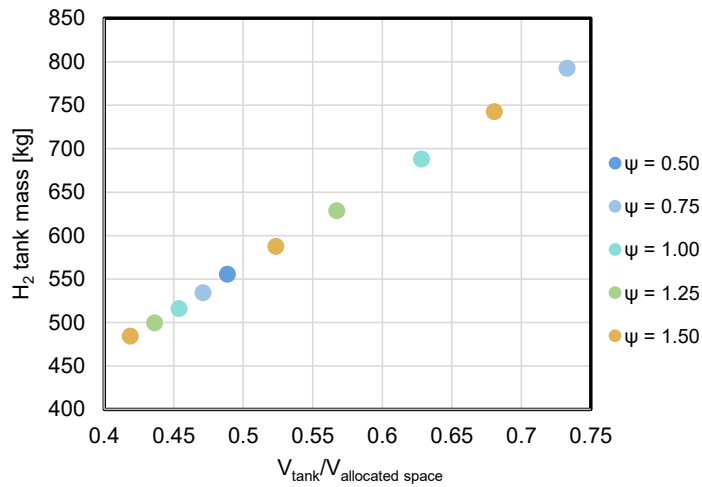
Figure 4.4: Tank of various shapes in a pre-defined allocated volume

Next, tanks of various shapes and volumes are analyzed for mass and space efficiency within a defined volume of 2m x 2m x 7.5m. The tanks are sized to contain a minimum of 345 kg of liquid hydrogen, and once again, the cross-section of the tanks has been fixed, and the geometrical ratios and overall shape of the tank were allowed to vary. Table 4.2 summarizes the assumptions of this study. Figure 4.5 presents the mass (figure 4.5a) and the gravimetric efficiency (figure 4.5b) for various tank shapes leading to different volumetric efficiencies. The tanks with low mass and, therefore, high gravimetric efficiency (defined in equation (25)) are also the ones having the lowest volumetric efficiencies. A trade-off between the mass and volume should, thus, drive the shape selection and require evaluation of aircraft-level impact.

$$\text{Gravimetric efficiency} = \frac{m_{\text{H}_2}}{m_{\text{H}_2} + m_{\text{tank}}} \quad (25)$$



(a) Tank mass vs. volumetric efficiency



(b) Gravimetric vs. volumetric efficiency

Figure 4.5: Impact of tank shape variation on the mass and gravimetric and volumetric efficiencies

Table 4.2: Assumptions in tank allocated space study

Variable	Value
Hydrogen mass [kg]	345
Allocated space dimensions [m]	$2 \times 2 \times 7.5$
Tank wall material	Al 2219
Material density [kg/m^3]	2840 [38]

A low volumetric efficiency means that the tank requires more storage space for a certain volume of hydrogen stored. A higher storage volume may require a fuselage extension, either in length or in diameter, which would increase the aerodynamic drag of the aircraft and impact the aircraft's performance. An alternative option would be to consider external storage configurations, such as wing-mounted pods. While this might not introduce the need for modifications of the fuselage, it would induce additional aerodynamic and structural challenges. Hence, the tank shape and placement have to take these factors into account to ensure the overall aircraft performance.

4.3 Tank Sizing Including Insulation

With the tank geometry defined, it is essential to consider the insulation needed to maintain cryogenic temperatures. Insulation plays a key role in preserving the hydrogen in a liquid state when the tank is exposed to ambient conditions for varying durations, minimizing the heat transfer and boil-off. This section explores different insulation materials and their impact on the overall tank geometry.

A study on different insulation materials for various durations of exposure to the ambient environment is done. The external temperature is set to represent on-ground conditions with a constant hot-day temperature throughout the exposure duration, resulting in conservative estimates. The required insulation thicknesses to maintain the hydrogen in a liquid state at cryogenic temperatures increase with exposure time, thus increasing the insulation mass. Figure 4.6 illustrates this mass increase for different insulation materials. The tank and its insulation are sized for 345 kg of hydrogen and a maximum design pressure of 10 bars [39]. Table 4.3 shows the assumptions for this study. The insulation material properties are listed in appendix B.

Table 4.3: Assumptions in tank sizing with insulation study

Variable	Value
Hydrogen mass [kg]	345
Design tank pressure [bar]	10
Outside temperature [$^{\circ}\text{C}$]	50

Insulation materials of the same type generally show similar trends, with the exception of cellular glass, which has a steeper mass-to-thickness slope, resulting in the heaviest configuration. For the same exposure time, the other foam insulations have masses ranging from 250 to 500 kg. While aerogels offer thinner insulation, they result in a higher mass than most foams due to their relatively higher density. Given that the hydrogen mass is 345 kg and the tank containing it (a tank with a 2.2 m diameter) is around 400 kg, insulation of this order of magnitude is preferable. Heavier insulation would not be suitable for aerospace applications. Figure 4.6 shows that, aside from some foams, in

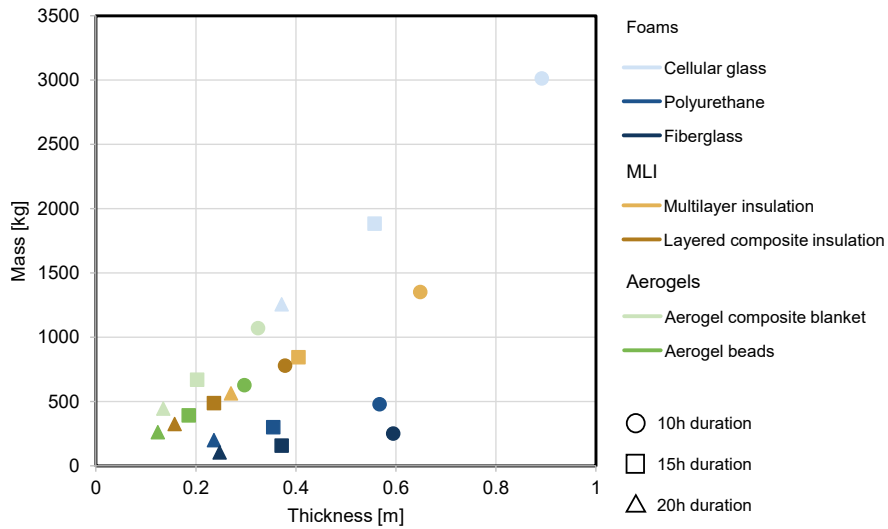


Figure 4.6: Tank and insulation mass for different insulation materials

the current configuration, most insulation options are unsuitable for long-term storage. However, foam-based insulation materials lead to an insulation thickness of above 0.5 m for the 2 m diameter tanks. Within a fixed aircraft fuselage diameter, the tank might need to be elongated to store the same amount of hydrogen, as space is taken up laterally by the insulation. This could necessitate a longer fuselage, adding to the aircraft’s weight and drag. Consequently, tanks with vacuum-based insulation should also be considered, as they offer a much lower thermal conductivity (and therefore a thinner insulation) compared to non-vacuum insulation.

To assess the variability of the insulation thickness and its impact on the tank length, a test case looking at the change of insulation and tank size with respect to exposure time was performed. The fuselage diameter remains fixed, and thus, the lateral space which can be taken by the tank is limited, while the tank length is allowed to vary. In this scenario, the tank diameter and the hydrogen mass remain constant, while the exposure duration at hot on-ground conditions is the varied parameter in the study. Figure 4.7 illustrates the configuration adopted for this case study, featuring a non-integral tank with allowances for attachments to the fuselage skin. The tank itself consists of a thin metal wall surrounded by insulation. Since the hydrogen mass and volume to be stored remain constant, increasing the insulation thickness reduces the available radial space for the tank, which in turn leads to the necessity of lengthening the tank to maintain the storage capacity.

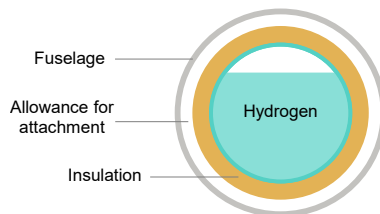
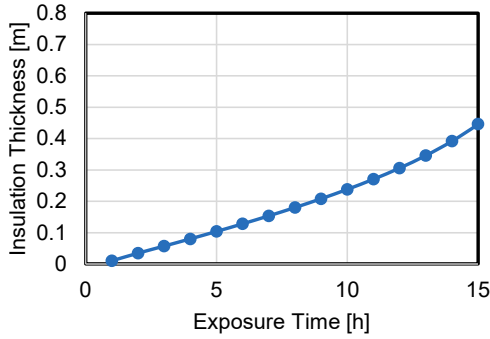
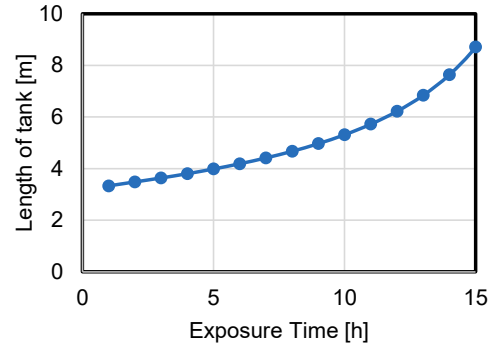


Figure 4.7: Fuselage cross-section with inserted hydrogen tank

Figure 4.8 shows the impact of the exposure duration on insulation thickness and the resulting length of the tank. Here, the study has been done with EPS insulation, a mid-range foam in terms of density and thermal conductivity properties. The longer the tank is exposed to high temperatures, the thicker the insulation required will be. As the tank is constrained by the fixed fuselage width, the tank's length also increases with exposure time.

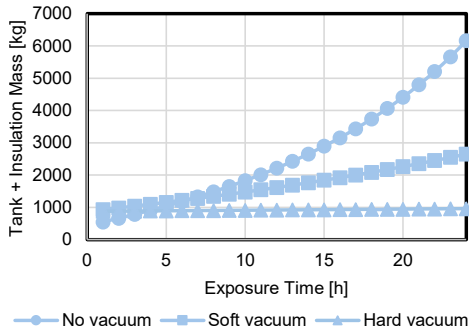


(a) Insulation thickness for different exposure times

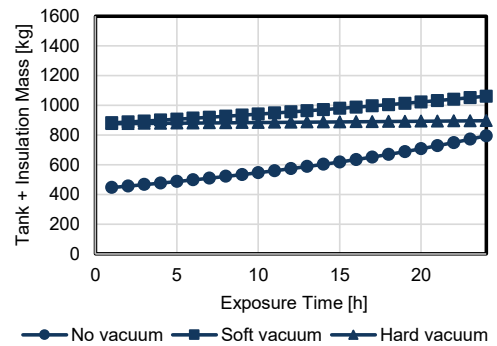


(b) Length of the tank for different exposure times

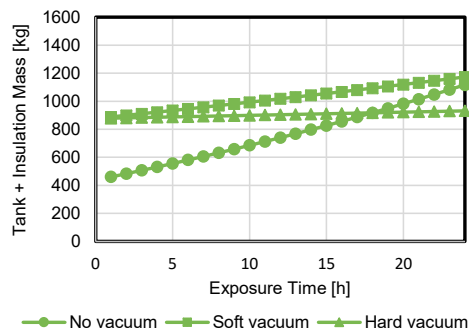
Figure 4.8: Impact of exposure time on insulation and tank sizing



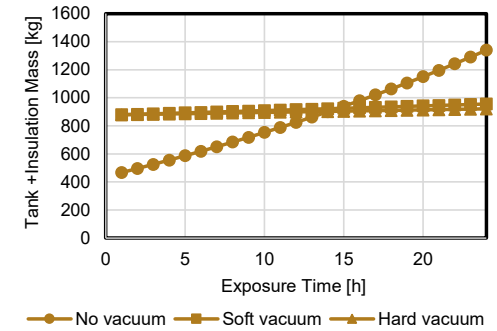
(a) Perlite



(b) Fiberglass



(c) Aerogel beads



(d) Layered composite insulation

Figure 4.9: Tank and insulation mass for varying exposure time (for different insulation materials)

The variation in thickness impacts not only the length of the tank but also its overall mass. Different insulation materials and types (non-vacuum and vacuum-based) result in different mass increase trends as exposure time increases. Figure 4.9 illustrates the overall tank mass for various insulation materials at different vacuum levels, where the two walls encompassing the vacuum are assumed to be identical. All materials exhibit a similar trend: non-vacuum insulation offers greater mass savings up to a certain exposure time. Beyond this point, vacuum-based insulation becomes more favourable, resulting in a lighter overall mass.

4.4 Multiple Tanks with Insulation and Fixed Mass of Hydrogen

This case study is conducted within the framework of the EAP collaborative project, which explores advanced propulsion solutions for next-generation business aircraft. Some of the architectures explored within the project are dual-fuel and all-electric configurations, as illustrated in 4.10. Both architectures would necessitate a hydrogen tank, whether the hydrogen is burned directly in an engine or is used in a fuel cell to generate electricity. Figure 4.11 illustrates some potential placements of the hydrogen tanks, which may lead to fuselage extension depending on the chosen configuration. The tanks' placement has to take into account the integration and compatibility with other already existing elements and systems onboard the aircraft, such as the APU and the Aft Equipment Bay (AEB) shown in figure 4.10. Some other key considerations for the tank placement are avoiding the rotor burst zone, ensuring appropriate placement relative to the Center of Gravity (CG) of the aircraft, and the accessibility of the tank for maintenance.

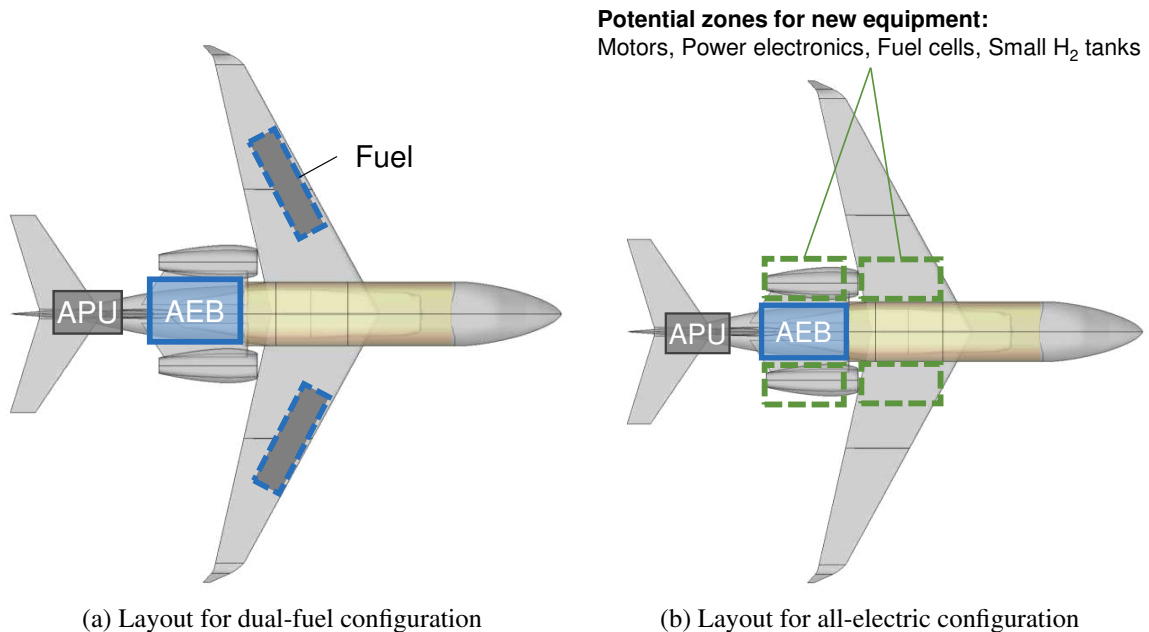


Figure 4.10: Notional layout of next-generation aircraft architectures

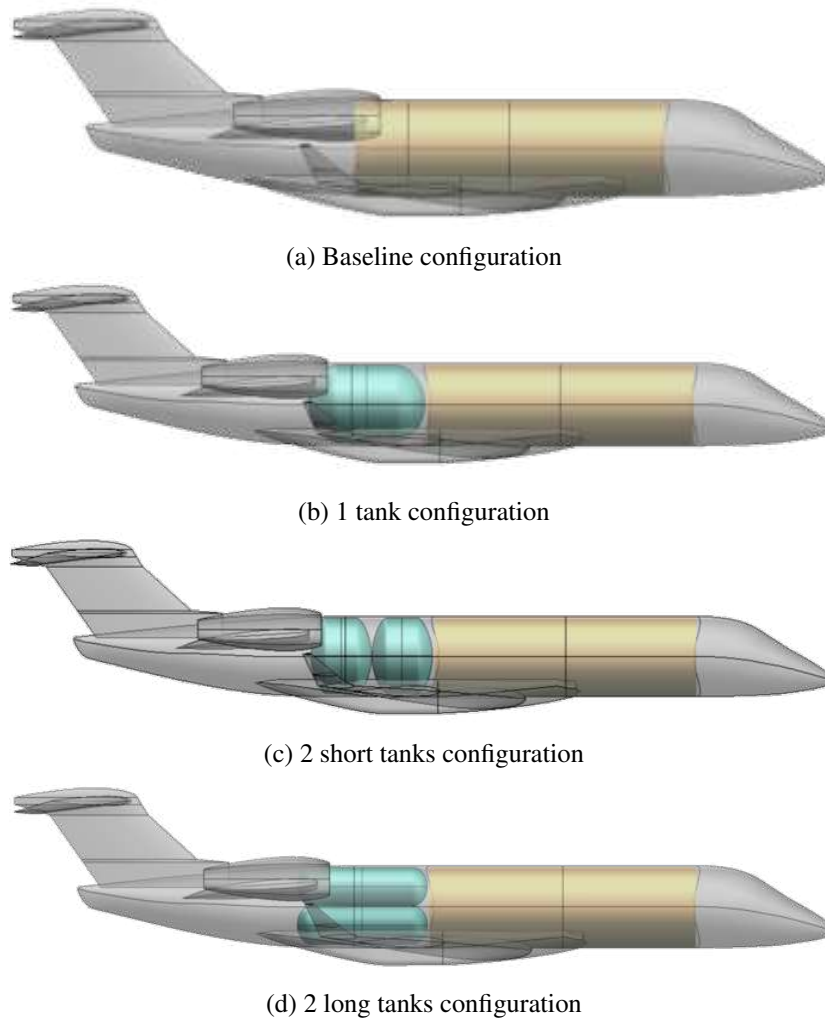


Figure 4.11: Hydrogen tanks placement configurations

The focus of this study is to size the cryogenic hydrogen storage tanks for a dual-fuel business aircraft design, achieving a mission range of up to 3000 nmi and transporting up to eight passengers. In this dual-fuel configuration, where the aircraft operates using both hydrogen and conventional jet-A fuel as propulsion energy sources, it was determined that the storage system has to be able to accommodate 345 kg of hydrogen. This serves as the requirement for the sizing and evaluation of the various tank layout configurations explored.

For safety considerations, multiple tanks may be necessary for storing hydrogen on the aircraft. In current aircraft, each engine must have its own independent fuel supply system and be fed fuel from a separate tank [40]; this will most likely also be a requirement for future aircraft. This requirement introduces redundancy, ensuring that if one tank is located in a risk zone, such as a rotor burst zone as illustrated in figure 4.12, or experiences a failure, the remaining tank(s) can continue to supply hydrogen, minimizing the risk of complete system failure. By distributing hydrogen storage across multiple tanks, the system is made more robust, enabling the remaining tank(s) to maintain functionality even in the event of a tank issue. This test case enables the exploration of various tank layouts and observes the impact on the system weight.

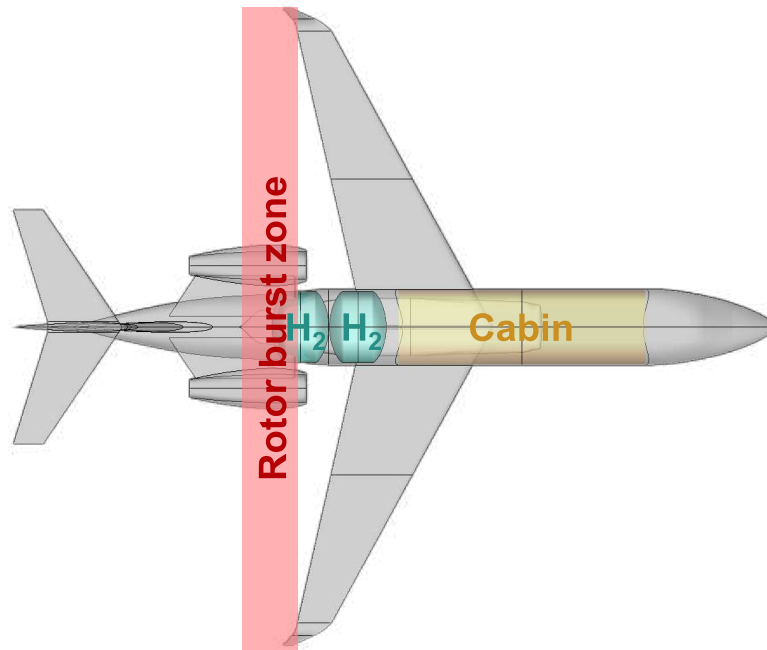


Figure 4.12: Illustration of notional engine rotor burst zone

Table 4.4 illustrates the different layouts explored in this test case, showing both transverse and longitudinal cross-sections of a notional fuselage. The layouts include configurations with 1 to 4 tanks and an arrangement with two shorter tanks occupying the entire cross-section of the fuselage. The characteristics of each of these layouts are also presented.

Table 4.4: Explored layouts definitions

	Layout schematic	Number of tanks	Tank diameter [m]
Layout 1		1	2.2
Layout 2		2	2.2
Layout 3		2	1.1
Layout 4		3	1.02
Layout 5		4	0.9

Tank layouts were sized for 345 kg of hydrogen with different insulation and at different vacuum levels. Table 4.5 summarizes the assumptions in this study. The tank structural weights are similar for the various configurations, however, the main impact is observed in the insulation weight, as illustrated in figure 4.13. The smaller, thinner tanks have a higher surface-to-volume ratio, making them more susceptible to boil-off, thus requiring thicker insulation. Inversely, in the second layout, rounder tanks require less insulation than their longer counterparts. The single tank configuration always leads to the lowest insulation mass due to its minimal surface area vs. volume ratio. However, as discussed previously, this might not necessarily be the optimal solution safety-wise. Generally, as the number of tanks increases, the insulation mass also increases. This is because the smaller tanks have a higher surface area to volume ratio, which increases the contact area with the environment and, thus, the need for insulation.

Table 4.5: Assumptions in multiple tank layouts study

Variable	Value
Hydrogen mass [kg]	345
Design tank pressure [bar]	10
Outside temperature [°C]	50
Exposure time [h]	10

The vacuum minimizes conduction and convection; therefore, to achieve the same level of thermal insulation, the thickness of the material would be thinner. When a material is subjected to hard vacuum, the insulation mass is significantly lower across all tank configurations compared to the soft and no-vacuum counterparts. This showcases the lower thermal conductivity and higher thermal efficiency of this type of insulation, requiring less material to achieve the needed thermal resistance to avoid boil-off. On the other hand, more material is needed to achieve the same thermal insulation without vacuum, which increases the overall mass.

The evaluation of various tank layouts in terms of placement and insulation type is an integral part of the sizing and design process. This study allows for the exploration of trade-offs between the tank configuration, insulation efficiency, and overall mass. In general, insulation subjected to hard vacuum provides a lighter solution across layouts due to its low thermal conductivity. In terms of the number of tanks, single-tank configurations are the ones with the smaller tank mass; however, they might not meet safety standards, as this type of configuration does not offer redundancy to the system. One of the other configurations, for example, the 2-big tanks or the 2-small tanks layouts, would have to be considered. A trade-off has to be done between the number of tanks and their associated mass, as multi-tank configurations induce mass penalties due to the increased surface area and, therefore, the increased insulation requirements. This case study underlines the need to explore various tank layout configurations and insulation methods to achieve a compromise between the number of tanks, the insulation efficiency and the overall mass of the system.

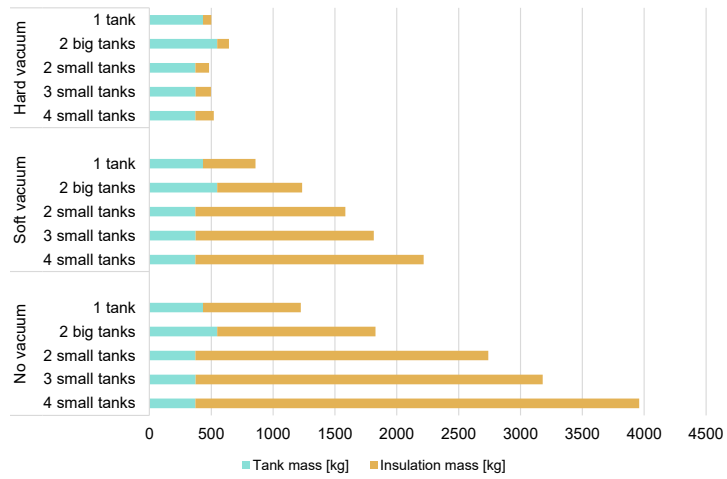
To evaluate a range of tank layouts for different potential hydrogen storage mass requirements spanning several orders of magnitude, similar studies were conducted for 50 kg and 1000 kg of hydrogen. These scenarios reflect use cases such as running only an APU on hydrogen or powering a substantial portion of the aircraft mission with hydrogen. The detailed results of these studies, including the mass, volume and geometrical parameters for each investigated combination of insulation materials, vacuum levels, and tank layouts, are provided in appendix E.

When selecting the tank configuration, several factors can be considered, such as the overall mass of the tanks, the volume they occupy, the diameter of the tank bundle, and its length. Table 4.6

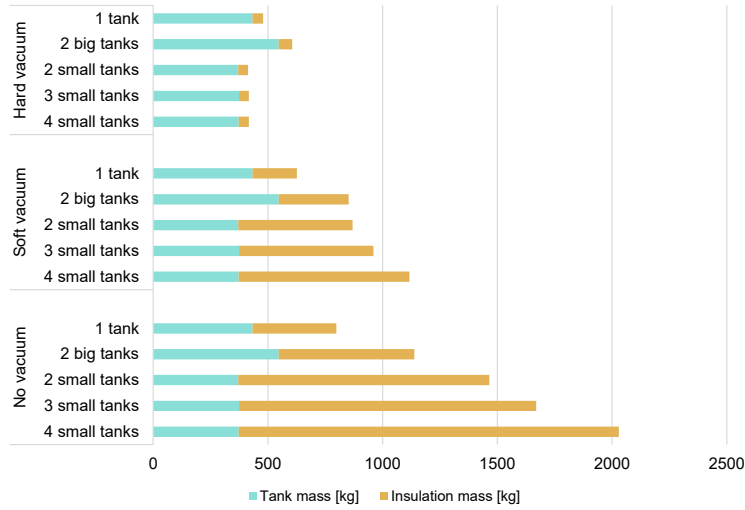
highlights the most advantageous tank configuration with respect to these factors for each hydrogen mass. For minimizing total mass and diameter, the configuration with two long tanks with MLI insulation under hard vacuum is the most favourable option. However, to minimize the fuselage length taken by the tanks, a single-tank configuration is preferred, whereas a three-tank layout offers the smallest overall occupied volume. These are consistent trends across all three tested hydrogen quantity configurations. The preferred tank configurations would depend on the relative importance given to each factor from an aircraft-level perspective.

Table 4.6: Preferred tank configurations based on various selection criteria

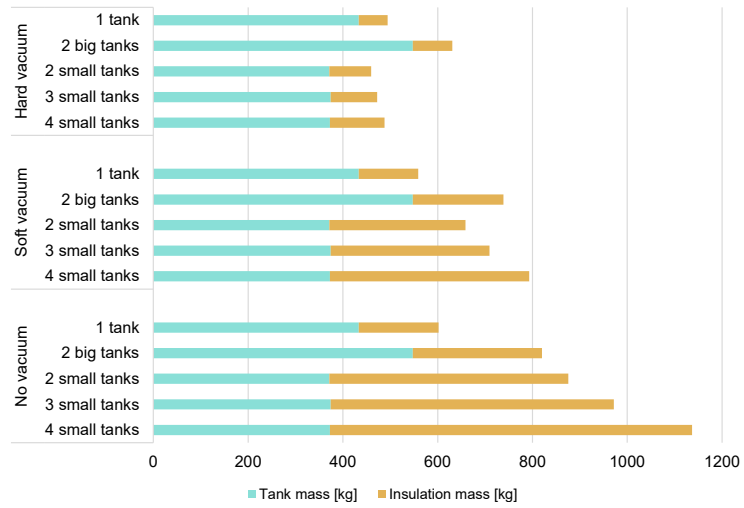
Hydrogen mass	Total mass	Diameter of tank bundle	Length	Occupied volume
50 kg	MLI hard vacuum 2 long tanks	MLI hard vacuum 2 long tanks	MLI hard vacuum 1 tank	MLI hard vacuum 3 tanks
345 kg	MLI hard vacuum 2 long tanks	MLI hard vacuum 2 long tanks	MLI hard vacuum 1 tank	MLI hard vacuum 3 tanks
1000 kg	MLI hard vacuum 2 long tanks	MLI hard vacuum 2 long tanks	MLI hard vacuum 1 tank	MLI hard vacuum 3 tanks



(a) Perlite



(b) Multilayer



(c) Aerogel beads

Figure 4.13: Tank and insulation weight for different tank layouts

4.5 Summary of Chapter 4

The test cases presented in this section showed that the geometrical shape of the tank has a significant impact on the mass and on the gravimetric and volumetric efficiency of the storage system. The type of insulation and the tanks' configuration also play a key role in the sizing and design process as they influence the resulting overall mass. The first test case showed that tanks with circular cross-sections, particularly spherical tanks, lead to the lowest mass for a given tank volume. Trade-off studies between the gravimetric efficiency and the volumetric efficiency are, however, needed as these tanks do not necessarily lead to the most efficient usage of space, as shown in the second case study. The developed model enables the evaluation of such trade-off studies. Another aspect of the tank sizing impacting the overall weight of the storage system is the insulation. It is influenced by the tank's exposure to the external environment as well as the size and, therefore, the surface area of the tank. Safety considerations in terms of placement within the aircraft and redundancy should also be taken into account, as this has an impact on the system layout and its total mass. Overall, the presented hydrogen tank sizing model provides a parametric and flexible approach to explore a variety of conceptual design requirements and variables for conventional and unconventional future aircraft configurations.

Chapter 5

Conclusion and Outlook

This thesis proposes a methodology to size cryogenic tanks for hydrogen storage parametrically. It aims to address the gaps in hydrogen tank sizing by developing a parametric methodology. It establishes an approach to size tanks of various geometries and volumes, considering the insulation needed to maintain the hydrogen at cryogenic temperatures. The critical parameters impacting the tank sizing were identified, and a flexible tool that supports variations in design parameters was implemented.

Literature focuses on stand-alone tank models or high-level models used in aircraft-level studies. Flexible and detailed tank models, which can be integrated into a [MDAO](#) environment and which allow the exploration of tank layout configurations, are yet to be explored. Typically, thermal analyses are performed with a selected insulation material and do not consider the amount of time the tank would be exposed to the environment. Overall, there is a lack of a highly parametric model that allows for the exploration of the variation of several geometrical, thermal, and environmental factors and their impact on the overall tank geometry.

Hence, the presented work develops a parametric model allowing the sizing of hydrogen tanks and their insulation while taking into account various design requirements.

5.1 Contributions

The contributions of this work include:

- The development of a parametric geometrical tank model supporting a variety of irregular tank shapes
- The calculation and integration into the sizing module of different boil-off allowance percentages
- The development of a time-dependent thermal module, taking into consideration the exposure time of the tank to the external environment
- The development of a flexible insulation module considering various insulation types and materials
- Addressing possible tank layout configurations within the airframe

5.2 Future Work

The hydrogen tank sizing tool developed in this thesis provides a foundation for further enhancements and integration in a broader design framework. Several areas for improvement can be identified regarding both the structural and the thermal aspects of the sizing methodology. Currently, the tool supports the design and sizing of ellipsoidal tanks of various lengths and eccentricities. Future work would accommodate even more unconventional tank shapes, such as truncated conical tanks to better allow for the insertion of a storage system into unconventionally shaped spaces, such as the tail of an aircraft. This would lead to the need for a more detailed analysis of the stresses to which the tank is subjected and the resulting structure. Additional thermal aspects, such as modelling the thermal stratification inside the tank and dynamic simulation of the temperature variations throughout the day, could also be incorporated, ultimately leading to more detailed and realistic insulation sizing. Simulating temperature fluctuations would enable the tool to account for varying environmental conditions, not only on ground but also throughout the mission of the aircraft. These tool improvements would add to the performance of the tool on the tank-sizing level and enhance the tool's capabilities on the aircraft level within an integrated framework, allowing for more advanced exploration of hydrogen-powered aircraft concepts.

In the future, the tank sizing tool will be integrated into a [MDAO](#) environment. This will allow the tool to be used in combination with other design modules and perform analysis on the aircraft level, including aircraft sizing and performance, particular risk and zonal safety analysis, and life cycle analysis. The integration of these tools will allow a more holistic exploration of future concepts of hydrogen-powered aircraft and ultimately facilitate the optimization of aircraft design and layout.

List of Related Publications

Conference Presentation

- G. Licheva, S. Liscouët-Hanke, *Cryogenic Tank Sizing Model for the Conceptual Design of Hydrogen Powered Aircraft*, Canadian Aeronautics and Space Institute (CASI) AERO Conference, 14-16 November 2023, Ottawa, ON, Canada

Conference Paper with Peer Review

- G. Licheva, S. Liscouët-Hanke, *Cryogenic Tank Sizing Model for The Conceptual Design of Hydrogen-Powered Aircraft*, International Council of the Aeronautical Sciences (ICAS) Congress, 9-13 September 2024, Florence, Italy

References

- [1] “Aviation Benefits Report,” International Civil Aviation Organization, Industry High Level Group Report, 2019.
- [2] “Executive Summary - Net Zero Roadmaps,” International Air Transport Association, Montreal, Canada, Tech. Rep. Executive Summary, 2023.
- [3] “NASA Aeronautics Strategic Implementation Plan 2019 Update,” National Aeronautics and Space Administration, Tech. Rep., 2019. [Online]. Available: www.nasa.gov
- [4] “Hydrogen Storage - Office of energy efficiency & renewable energy.” [Online]. Available: <https://www.energy.gov/eere/fuelcells/hydrogen-storage>
- [5] C. O. Colpan and A. Kovač, *Fuel Cell and Hydrogen Technologies in Aviation*, ser. Sustainable Aviation. Cham: Springer International Publishing, 2022. [Online]. Available: <https://link.springer.com/10.1007/978-3-030-99018-3>
- [6] G. D. Brewer, *Hydrogen Aircraft Technology*, 1st ed. United States: CRC Press, Inc., 1991. [Online]. Available: <https://www.taylorfrancis.com/books/9781351439794>
- [7] S. K. Mital, J. Z. Gyekenyesi, R. Engineering, S. M. Arnold, R. M. Sullivan, J. M. Manderscheid, and P. L. N. Murthy, “Review of Current State of the Art and Key Design Issues With Potential Solutions for Liquid Hydrogen Cryogenic Storage Tank Structures for Aircraft Applications,” 2006.
- [8] E. J. Adler and J. R. Martins, “Hydrogen-powered aircraft: Fundamental concepts, key technologies, and environmental impacts,” *Progress in Aerospace Sciences*, vol. 141, p. 100922, Aug. 2023. [Online]. Available: <https://linkinghub.elsevier.com/retrieve/pii/S0376042123000386>
- [9] M. Aziz, “Liquid Hydrogen: A Review on Liquefaction, Storage, Transportation, and Safety,” *Energies*, vol. 14, no. 18, p. 5917, Sep. 2021. [Online]. Available: <https://www.mdpi.com/1996-1073/14/18/5917>
- [10] T. Amirthan and M. Perera, “The role of storage systems in hydrogen economy: A review,” *Journal of Natural Gas Science and Engineering*, vol. 108, p. 104843, Dec. 2022. [Online]. Available: <https://linkinghub.elsevier.com/retrieve/pii/S1875510022004292>
- [11] A. Goldmann, W. Sauter, M. Oettinger, T. Kluge, U. Schröder, J. Seume, J. Friedrichs, and F. Dinkelacker, “A Study on Electrofuels in Aviation,” *Energies*, vol. 11, no. 2, p. 392, Feb. 2018. [Online]. Available: <https://www.mdpi.com/1996-1073/11/2/392>

- [12] G. D. Brewer, R. E. Morris, R. H. Lange, and J. W. Moore, “Summary Report: Study of the Application of Hydrogen Fuel to Long-range Subsonic Transport Aircraft (Volume I),” Lockheed Aircraft Corporation, USA, Summary Report NASA CR-132558, Jan. 1975.
- [13] G. D. Brewer and R. E. Morris, “Study of LH2 Fueled Subsonic Passenger Transport Aircraft,” Lockheed Aircraft Corporation, USA, Final Report NASA CR-144935, Jan. 1976.
- [14] H. G. Klug and R. Faass, “CRYOPLANE: hydrogen fuelled aircraft — status and challenges,” *Air & Space Europe*, vol. 3, no. 3-4, pp. 252–254, May 2001. [Online]. Available: <https://linkinghub.elsevier.com/retrieve/pii/S1290095801901108>
- [15] H. Pohl and V. Malychev, “Hydrogen in future civil aviation,” *International Journal of Hydrogen Energy*, vol. 22, no. 10-11, pp. 1061–1069, Oct. 1997. [Online]. Available: <https://linkinghub.elsevier.com/retrieve/pii/S0360319995001409>
- [16] K. Barabanova, “ZeroAvia Flight Testing Hydrogen-Electric Powerplant,” Jan. 2023. [Online]. Available: <https://zeroavia.com/flight-testing/>
- [17] “Airbus reveals new zero-emission concept aircraft | Airbus,” Oct. 2021, section: Sustainability. [Online]. Available: <https://www.airbus.com/en/newsroom/press-releases/2020-09-airbus-reveals-new-zero-emission-concept-aircraft>
- [18] “Projects - EAP: Exploration and modeling of alternative propulsion technologies for business jets.” [Online]. Available: <https://www.criaq.aero/en/projects/>
- [19] D. Verstraete, “The Potential of Liquid Hydrogen for long range aircraft propulsion,” Ph. D. Thesis, Cranfield University, Apr. 2009.
- [20] D. Verstraete, P. Hendrick, P. Pilidis, and K. Ramsden, “Hydrogen fuel tanks for subsonic transport aircraft,” *International Journal of Hydrogen Energy*, vol. 35, no. 20, pp. 11 085–11 098, Oct. 2010. [Online]. Available: <https://linkinghub.elsevier.com/retrieve/pii/S036031991001236X>
- [21] C. Winnefeld, T. Kadyk, B. Bensmann, U. Krewer, and R. Hanke-Rauschenbach, “Modelling and Designing Cryogenic Hydrogen Tanks for Future Aircraft Applications,” *Energies*, vol. 11, no. 1, p. 105, Jan. 2018. [Online]. Available: <http://www.mdpi.com/1996-1073/11/1/105>
- [22] V. K. Mantzaroudis and E. E. Theotokoglou, “Computational Analysis of Liquid Hydrogen Storage Tanks for Aircraft Applications,” *Materials*, vol. 16, no. 6, p. 2245, Mar. 2023. [Online]. Available: <https://www.mdpi.com/1996-1944/16/6/2245>
- [23] V. Palladino, A. Jordan, N. Bartoli, P. Schmollgruber, V. Pommier-Budinger, and E. Benard, “Preliminary studies of a regional aircraft with hydrogen-based hybrid propulsion,” in *AIAA Aviation 2021 Forum*. American Institute of Aeronautics and Astronautics, Inc., Jul. 2021.
- [24] A. J. Colozza, “Hydrogen Storage for Aircraft Applications Overview,” Glenn Research Center, Analex Corporation, Brook Park, Ohio , USA, Contractor Report NASA/CR-2002-211867, Sep. 2002.
- [25] A. Gomez and H. Smith, “Liquid hydrogen fuel tanks for commercial aviation: Structural sizing and stress analysis,” *Aerospace Science and Technology*, vol. 95, p. 105438, Dec. 2019. [Online]. Available: <https://linkinghub.elsevier.com/retrieve/pii/S1270963818304139>

- [26] K. Shank, B. Thomas, and R. K. Agarwal, “Insulation Design for Liquid Cryogenic Hydrogen Fuel Tanks for Hydrogen Powered Aircraft,” in *AIAA Aviation 2023 Forum*. San Diego, CA and Online: American Institute of Aeronautics and Astronautics, Jun. 2023. [Online]. Available: <https://arc.aiaa.org/doi/10.2514/6.2023-3803>
- [27] S. Sarkar, G. Grandi, and S. Patel, “Hydrogen Fuel System for Aircraft,” Fort Worth, Texas, United States, Mar. 2023, pp. 2023–01–0976. [Online]. Available: <https://www.sae.org/content/2023-01-0976>
- [28] G. Onorato, P. Proesmans, and M. F. M. Hoogreef, “Assessment of hydrogen transport aircraft: Effects of fuel tank integration,” *CEAS Aeronautical Journal*, vol. 13, no. 4, pp. 813–845, Oct. 2022. [Online]. Available: <https://link.springer.com/10.1007/s13272-022-00601-6>
- [29] K. Alsamri, J. J. De la Cruz, M. Emmanouilidi, J. L. Huynh, and J. Brouwer, “Methodology to Assess Emissions and Performance Trade-Offs for a Retrofitted Solid Oxide Fuel Cell Hybrid and Hydrogen Powered Aircraft,” in *AIAA SciTech 2023 Forum*. National Harbor, MD & Online: American Institute of Aeronautics and Astronautics, Jan. 2023. [Online]. Available: <https://arc.aiaa.org/doi/10.2514/6.2023-1954>
- [30] R. D. McCarty, J. Hord, and . M. Roder, *Selected properties of hydrogen (engineering design data)*. Washington, US: US Department of Commerce, Feb. 1981.
- [31] Y. A. Çengel and M. A. Boles, *Thermodynamics: an engineering approach*, 8th ed. New York, NY: McGraw-Hill Education, 2015.
- [32] Tirupathi R. Chandrupatla and Thomas J. Osler, “The Perimeter of an ellipse,” *Mathematical Scientist*, vol. 35, pp. 122–131, 2010, publisher: Applied Probability Trust.
- [33] Gérard P. Michon, “Surface Area of an Ellipsoid - Scalene Ellipsoid,” Apr. 2020. [Online]. Available: <https://www.numericana.com/answer/ellipsoid.htm#thomsen>
- [34] S. D. Augustynowicz, J. E. Fesmire, and J. P. Wikstrom, “Cryogenic Insulation Systems,” Sydney, 1999.
- [35] J. E. Fesmire and a. D. Augustynowicz, “Cryogenic Thermal Insulation Systems,” Orlando, FL, 2005, cryogenics Test Laboratory NASA Kennedy Space Center. [Online]. Available: <https://tfaws.nasa.gov/TFAWS05/Website/files/Cryogenic%20Insulation%20Technology.pdf>
- [36] F. P. Incropera, D. P. DeWitt, T. L. Bergman, and A. S. Lavine, Eds., *Fundamentals of heat and mass transfer*, 6th ed. Hoboken, NJ: Wiley, 2007.
- [37] Linde Group, “Cryogenic Standard Tanks - LITS 2.” [Online]. Available: https://assets.linde.com/-/media/global/engineering/engineering/home/products-and-services/plant-components/cryogenic-tanks/p_3_3_e_12_150dpi.pdf
- [38] K. Anderson, J. Weritz, and J. G. Kaufman, *Properties and selection of aluminum alloys*. ASM International, Jun. 2019. [Online]. Available: <https://doi.org/10.31399/asm.hb.v02b.9781627082105>
- [39] Friedel Michel, “Cryogenic Reservoirs,” in *Hydrogen Technology: Mobile and Portable Applications*, 1st ed. Germany: Springer, 2008.

- [40] “14 CFR Part 25 Subpart E - Fuel System,” Sep. 2018. [Online]. Available: <https://www.ecfr.gov/current/title-14/part-25/subject-group-ECFRa93e11eb94bb0c1>
- [41] G. Maragkos and T. Beji, “Review of Convective Heat Transfer Modelling in CFD Simulations of Fire-Driven Flows,” *Applied Sciences*, vol. 11, no. 11, p. 5240, Jun. 2021. [Online]. Available: <https://www.mdpi.com/2076-3417/11/11/5240>
- [42] S. W. Churchill and H. H. Chu, “Correlating equations for laminar and turbulent free convection from a horizontal cylinder,” *International Journal of Heat and Mass Transfer*, vol. 18, no. 9, pp. 1049–1053, Sep. 1975. [Online]. Available: <https://linkinghub.elsevier.com/retrieve/pii/0017931075902227>
- [43] “Mechanical properties of carbon and alloy steels,” in *Metals handbook desk edition*, J. Davis, Ed. ASM International, 1998, pp. 219–225. [Online]. Available: <https://dl.asminternational.org/handbooks/edited-volume/chapter-pdf/522370/a0003093.pdf>
- [44] G. R. C. Jr., *Hydrogen compatibility handbook for stainless steels*. Aiken, SC: E. I. du Pont de Nemours & Co., Savannah River Laboratory, 1983. [Online]. Available: <https://www.osti.gov/servlets/purl/5906050>

Appendix A

Hydrogen Tank Sizing Equations Derivations

This section shows the detailed derivations of the equations used in the tank sizing process.

A.1 Hydrogen Properties

This subsection focuses on the equations derived for the determination of the tank volume in section 3.2.

From equation (2), equation (4) is derived in the following manner:

$$\nu_{\text{avg}} = \nu_f + x \nu_{fg} \quad (2)$$

$$\nu_{\text{avg}} = \nu_f + x (\nu_g - \nu_f)$$

$$\frac{1}{\rho_{\text{avg}}} = \frac{1}{\rho_f} + x \left(\frac{1}{\rho_g} - \frac{1}{\rho_f} \right)$$

$$\rho_{\text{avg}} = \frac{1}{\frac{1}{\rho_f} + x \left(\frac{1}{\rho_g} - \frac{1}{\rho_f} \right)}$$

$$\rho_{\text{avg}} = \frac{1}{\frac{\rho_g}{\rho_g \rho_f} + \frac{x \rho_f}{\rho_g \rho_f} - \frac{x \rho_g}{\rho_g \rho_f}}$$

$$\rho_{\text{avg}} = \frac{1}{\frac{\rho_g + x \rho_f - x \rho_g}{\rho_g \rho_f}}$$

$$\rho_{\text{avg}} = \frac{\rho_g \rho_f}{\rho_g + x \rho_f - x \rho_g} \quad (4)$$

Using the following relations:

$$y = \frac{V_l}{V_t} \quad V_l = V_t y \quad V_g = V_t (1 - y) \quad m = \rho V$$

and building upon equation (3), first the quality x in terms of y is obtained:

$$x = \frac{m_g}{m_f + m_g} \quad (3)$$

$$x = \frac{\rho_g V_g}{\rho_g V_g + \rho_f V_f}$$

$$x = \frac{\rho_g V_t (1 - y)}{\rho_g V_t (1 - y) + \rho_f V_t y}$$

$$x = \frac{\rho_g (1 - y)}{\rho_g (1 - y) + \rho_f y} \quad (5)$$

Combining equations: (4) and (5), the equation of average pressure in terms of y can be obtained:

$$\rho_{avg} = \frac{\rho_g \rho_f}{x (\rho_f - \rho_g) + \rho_g}$$

$$\rho_{avg} = \frac{\rho_g \rho_f}{\left(\frac{\rho_g (1 - y)}{\rho_g (1 - y) + \rho_f y} \right) (\rho_f - \rho_g) + \rho_g} \quad (6)$$

From equation (6), equation (7) is derived in the following manner:

$$\rho_{avg} = \frac{\rho_g \rho_f}{\left(\frac{\rho_g (1 - y)}{\rho_g (1 - y) + \rho_f y} \right) (\rho_f - \rho_g)} \quad (6)$$

$$\rho_{avg} = \frac{\rho_g \rho_f}{\left(\frac{\rho_g (1 - y) (\rho_f - \rho_g)}{\rho_g (1 - y) + \rho_f y} \right) + \rho_g}$$

$$\frac{1}{\rho_{avg}} = \frac{\left(\frac{\rho_g (1 - y) (\rho_f - \rho_g)}{\rho_g (1 - y) + \rho_f y} \right) + \rho_g}{\rho_g \rho_f}$$

$$\frac{\rho_g \rho_f}{\rho_{avg}} = \rho_g + \frac{\rho_g (1 - y) (\rho_f - \rho_g)}{\rho_g (1 - y) + \rho_f y}$$

$$\frac{\rho_g \rho_f}{\rho_{avg}} = \frac{(-\rho_g + \rho_g y - \rho_f y) \rho_g - [\rho_g (1 - y) (\rho_f - \rho_g)]}{-\rho_g + \rho_g y + \rho_f y}$$

$$\frac{\rho_g \rho_f}{\rho_{avg}} = \frac{(-\rho_g + \rho_g y - \rho_f y) \rho_g - [\rho_g \rho_f - \rho_g^2 - \rho_g \rho_f y + \rho_g^2 y]}{-\rho_g + \rho_g y + \rho_f y}$$

$$\frac{\rho_g \rho_f}{\rho_{avg}} = \frac{-\rho_g^2 + \rho_g^2 y - \rho_f \rho_g y - \rho_g \rho_f + \rho_g^2 + \rho_g \rho_f y - \rho_g^2 y}{-\rho_g + \rho_g y + \rho_f y}$$

$$\frac{\rho_g \rho_f}{\rho_{avg}} = -\frac{\rho_g \rho_f}{-\rho_g + \rho_g y + \rho_f y}$$

$$\frac{\rho_{avg}}{\rho_g \rho_f} = -\frac{-\rho_g + \rho_g y + \rho_f y}{\rho_g \rho_f}$$

$$-\frac{\rho_g \rho_f \rho_{avg}}{\rho_g \rho_f} = -\rho_g + \rho_g y + \rho_f y$$

$$-\rho_{avg} = y(-\rho_f + \rho_g) - \rho_g$$

$$y(-\rho_f + \rho_g) = \rho_g - \rho_{avg}$$

$$y = \frac{\rho_g - \rho_{avg}}{\rho_g - \rho_f} \quad (7)$$

A.2 Insulation Sizing

This subsection describes the equations leading to the definition of the convection heat transfer coefficient and ultimately to the thermal resistance for convection given by equation (20).

Grashof number (Gr) is the ratio of the buoyancy forces to the viscous forces acting on a fluid and is defined as follows [36]:

$$\text{Gr} = \frac{g \cdot \beta \cdot (T_{\text{surf}} - T_{\infty}) \cdot L^3}{\nu^2} \quad (26)$$

where β is the volumetric thermal expansion:

$$\beta = \frac{1}{T_{\infty}} \quad (27)$$

The Prandtl number (Pr) is a measure of the relationship between momentum diffusivity and thermal diffusivity [36]:

$$\text{Pr} = \frac{C_p \cdot \mu}{k_{\text{air}}} \quad (28)$$

from these two numbers, the Rayleigh number (Ra) can be calculated [36]:

$$\text{Ra} = \text{Gr} \cdot \text{Pr} \quad (29)$$

The Nusselt number (Nu) is the ratio of convection to pure conduction heat transfer convection and can be defined as [36]:

$$\text{Nu} = \frac{hL}{k} \quad (30)$$

Empirical correlations have been defined for the Nusslet number depending on the geometry of the object in the fluid, as well as the conditions of the convection (natural or forced). Below are the Nusselt number equations for natural convection over a sphere and a cylinder, respectively.

Nusselt number for natural convection over a sphere [41]:

$$\text{Nu} = 2 + \frac{0.589 \text{Ra}^{1/4}}{\left(1 + \left(\frac{0.469}{\text{Pr}}\right)^{9/16}\right)^{4/9}} \quad (31)$$

Nusselt number for natural convection over a horizontal cylinder [42]:

$$\text{Nu} = \left(0.60 + \frac{0.387 \text{Ra}^{1/6}}{\left(1 + \left(\frac{0.559}{\text{Pr}}\right)^{9/16}\right)^{8/27}}\right)^2 \quad (32)$$

Once the Nusselt number is calculated, equation (30) can be rearranged to determine the convection heat transfer coefficient.

$$h = \frac{k \cdot \text{Nu}}{L} \quad (33)$$

Appendix B

Insulation Materials Properties

The following are the properties of the insulation materials considered in this thesis:

Table B.1: Insulation materials properties (adapted from [26], [34], [35])

	Material	Density [kg/m ³]	k-value [mW/m·K] No vacuum	k-value [mW/m·K] Soft vacuum	k-value [mW/m·K] High vacuum
Foams	Cellular glass	128	33	-	-
	Perlite	128	32	16	1 - 1.5
	Expanded polystyrene	26	26	-	-
	Polyurethane	32	21	-	-
	Fiberglass	16	22	14	2
Multilayer insulation	Multilayer insulation	79	24	10	0.09
	Layered composite insulation	78	14	1.6	0.09
Aerogels	Aerogel composite blanket	125	12	3.4	0.5 - 0.6
	Aerogel beads	80	11	5.4	1.1

Note: No vacuum is considered to be 760 torr, soft vacuum is 1 torr, and hard vacuum is $< 10^{-5}$ torr.

Appendix C

Tank Geometrical Parameters Solver

Here is the full implementation of the geometrical solver in the hydrogen tank sizing tool.

```
1 def solve_variables(known_values):
2     if known_values['a_i'] < 0:
3         a = sp.symbols('a')
4         known_values['a_i'] = a
5     else:
6         a = (known_values['a_i'])
7
8     if known_values['b_i'] < 0:
9         b = sp.symbols('b')
10        known_values['b_i'] = b
11    else:
12        b = (known_values['b_i'])
13
14    if known_values['c_i'] < 0:
15        c = sp.symbols('c')
16        known_values['c_i'] = c
17    else:
18        c = (known_values['c_i'])
19
20    if known_values['l_s_i'] < 0:
21        l_s = sp.symbols('l_s')
22        known_values['l_s_i'] = l_s
23    else:
24        l_s = (known_values['l_s_i'])
25
26    if known_values['l_t_i'] < 0:
27        l_t = sp.symbols('l_t')
28        known_values['l_t_i'] = l_t
29    else:
30        l_t = (known_values['l_t_i'])
31
32    if known_values['phi_i'] < 0:
33        phi = sp.symbols('phi')
34        known_values['phi_i'] = phi
35    else:
36        phi = (known_values['phi_i'])
37
38    if known_values['psi_i'] < 0:
39        psi = sp.symbols('psi')
```

```

40     known_values['psi_i'] = psi
41 else:
42     psi = (known_values['psi_i'])
43
44 if known_values['lambda__i'] < 0:
45     lambda_ = sp.symbols('lambda_')
46     known_values['lambda__i'] = lambda_
47 else:
48     lambda_ = (known_values['lambda__i'])
49
50 if known_values['V_t_i'] < 0:
51     V_t = sp.symbols('V_t')
52     known_values['V_t_i'] = V_t
53 else:
54     V_t = (known_values['V_t_i'])
55 print('known_values after if statements', known_values)
56
57 # Identify unknown variables based on the known values
58 unknown_variables = [sp.symbols(symbol[:-2]) for symbol, value in
59 \ known_values.items() if not sp.sympify(value).is_number]
60 print('unknown_variables', unknown_variables)
61
62 # Define the equations
63 equations = [
64     sp.Eq(sp.pi*a*c*l_s + (4/3)*sp.pi*a*b*c, V_t),
65     sp.Eq(a/c, phi),
66     sp.Eq(b/c, psi),
67     sp.Eq(l_s/l_t, lambda_),
68     sp.Eq(l_s + 2*b, l_t)
69 ]
70
71 # Substitute known values into the equations
72 equations_with_values = [equation.subs(known_values) for equation in
73 \ equations]
74 print('equations', equations_with_values)
75
76 # Solve the system of equations for the remaining variables
77 solution_raw = sp.solve(equations_with_values, unknown_variables,
78 \ real=True)
79 if solution_raw == []:
80     print('There is no solution')
81     exit()
82 else:
83     print(f'THE SOLUTION IS {solution_raw}')
84
85 solution = []
86 if isinstance(solution_raw, dict):
87     # If the solutions are in dictionary format, convert to a list of
88     \ tuples
89     solution_tuples = tuple(solution_raw[var] for var in unknown_variables)
90     solution.append(solution_tuples)
91 elif isinstance(solution_raw, list):
92     # If the solutions are already in list format, use them directly
93     solution.extend(solution_raw)
94
95 # This identifies the number of elements that are part of a real solution
96 real_num = 0

```

```

93     for tuple_ in solution:
94         for element in tuple_:
95             if isinstance(element, sp.core.numbers.Float):
96                 real_num += 1
97
98     # This calculates the number of real solutions (set of parameters)
99     sol_row = int((real_num)/len(unknown_variables))
100     # Initialize solution matrix
101     compl_sol = np.zeros([sol_row, 9])
102     # Creates a matrix where the solutions are to be stored
103     sol_matrix = np.zeros((sol_row, len(unknown_variables)))
104
105     # Stores the real solution elements/variables into the solution matrix
106     for row in range(sol_row):
107         for tuple_ in solution:
108             i = 0
109             for element in tuple_:
110                 if isinstance(element, sp.core.numbers.Float):
111                     sol_matrix[row, i] = solution[row][i]
112                     i += 1
113
114     print('sol_matrix matrix', sol_matrix)
115     print('unknown_variable matrix', unknown_variables)
116     print('known_values dictionary', known_values)
117
118     # Assigning variable values to the complete solution matrix
119     for i in range(sol_row):
120         if a in unknown_variables: # Is the variable in the unknown values
121             compl_sol[i, 0] = sol_matrix[i, unknown_variables.index(a)]
122         else:
123             compl_sol[i, 0] = known_values['a_i']
124
125         if b in unknown_variables: # Is the variable in the unknown values
126             compl_sol[i, 1] = sol_matrix[i, unknown_variables.index(b)]
127         else:
128             compl_sol[i, 1] = known_values['b_i']
129
130         if c in unknown_variables: # Is the variable in the unknown values
131             compl_sol[i, 2] = sol_matrix[i, unknown_variables.index(c)]
132         else:
133             compl_sol[i, 2] = known_values['c_i']
134
135         if l_s in unknown_variables: # Is the variable in the unknown values
136             compl_sol[i, 3] = sol_matrix[i, unknown_variables.index(l_s)]
137         else:
138             compl_sol[i, 3] = known_values['l_s_i']
139
140         if l_t in unknown_variables: # Is the variable in the unknown values
141             compl_sol[i, 4] = sol_matrix[i, unknown_variables.index(l_t)]
142         else:
143             compl_sol[i, 4] = known_values['l_t_i']
144
145         if phi in unknown_variables: # Is the variable in the unknown values
146             compl_sol[i, 5] = sol_matrix[i, unknown_variables.index(phi)]
147         else:
148             compl_sol[i, 5] = known_values['phi_i']
149

```

```

150     if psi in unknown_variables: # Is the variable in the unknown values
151         compl_sol[i, 6] = sol_matrix[i, unknown_variables.index(psi)]
152     else:
153         compl_sol[i, 6] = known_values['psi_i']
154
155     if lambda_ in unknown_variables: # Is the variable in the unknown
156         \ values
157         compl_sol[i, 7] = sol_matrix[i, unknown_variables.index(lambda_)]
158     else:
159         compl_sol[i, 7] = known_values['lambda__i']
160
161     if V_t in unknown_variables: # Is the variable in the unknown values
162         compl_sol[i, 8] = sol_matrix[i, unknown_variables.index(V_t)]
163     else:
164         compl_sol[i, 8] = known_values['V_t_i']
165 print(compl_sol, '\n')
return compl_sol

```

Appendix D

Hydrogen Tank Validation Assumptions

Table D.1 compiles the geometrical parameters from datasheets [37] of the tanks used in the tool validation process.

Table D.1: Geometrical parameters for cryogenic tanks

Tank diameter [mm]	Tank height [mm]	Tank weight [kg]
1600	4150	2510
1600	7150	4910
2000	7350	5940
2400	8350	9840
2400	11550	13920
3000	11550	19300
3000	14150	23370
3000	18050	29650

Table D.2 outlines the materials and the assumed properties of the tank walls and insulation used in the validation process.

Table D.2: Material properties for the validation cases (from [43], [34], [44])

	Material	Pressure [Pa]	Density [kg/m ³]	Stress [Pa]	Young's modulus [Pa]	Thermal conductivity [W/m · K]
Inner vessel	austenitic steel	1.8×10^6	7850	230×10^6	209×10^9	14
Insulation	perlite powder	500	128	-	-	0.016
Outer vessel	carbon steel	-	7801	415×10^6	215×10^9	43

Finally, table D.3 summarizes the assumed hydrogen conditions in the tank for the validation cases.

Table D.3: Hydrogen conditions for the validation cases

Pressure [bar]	liquid level at boil-off conditions [%]	Hold time [h]
18	95	24

Appendix E

Tank Layouts Characteristics Data

Tables E.1 to E.3 present the detailed data from the study conducted as part of the case study described in section 4.4.

The tables use a colour-coded gradient scheme where green represents the most desirable results (lowest mass, smallest diameter, shortest length, and lowest volume) and orange indicates the least desirable results. The most advantageous values are also highlighted in bold for clarity.

In the tables:

- The *Diameter of tank bundle* refers to the overall diameter after arranging the tanks in their circular layout configuration (as seen in the layout schematic section in table 4.6)
- The *Length* is the total length of the tank configuration
- The *Volume* is the volume that would be necessary to encapsulate the entire bundle.

Table E.1: Tank integration characteristics for 50 kg mass of hydrogen

Vacuum level	Insulation material	Number of tanks	Total mass	Diameter of tank bundle	Length	Volume
No vacuum	Perlite	4	1160	3.56	2.32	29.43
		3	993	2.87	2.22	18.29
		2 (long)	744	2.37	2.22	12.43
		2 (large)	3231	4.86	5.79	136.72
		1	1077	3.67	1.95	26.32
	MLI	4	578	2.98	1.92	17.09
		3	503	2.45	1.85	11.06
		2 (long)	384	2.05	1.90	7.97
		2 (large)	1661	4.19	4.46	78.35
		1	591	3.30	1.58	17.22
	Aerogel beads	4	309	2.05	1.26	5.32
		3	276	1.76	1.25	3.86
		2 (long)	217	1.53	1.38	3.24
		2 (large)	935	3.11	2.29	22.20
		1	366	2.70	0.98	7.14
Soft vacuum	Perlite	4	661	2.39	1.49	8.51
		3	569	2.00	1.46	5.85
		2 (long)	429	1.71	1.56	4.58
		2 (large)	1920	3.51	3.09	38.04
		1	663	2.92	1.19	10.12
	MLI	4	311	1.97	1.20	4.63
		3	278	1.69	1.19	3.41
		2 (long)	218	1.48	1.33	2.92
		2 (large)	963	3.02	2.11	19.16
		1	377	2.65	0.92	6.44
	Aerogel beads	4	206	1.65	0.97	2.63
		3	191	1.45	0.99	2.09
		2 (long)	156	1.31	1.15	1.96
		2 (large)	675	2.64	1.35	9.43
		1	291	2.44	0.71	4.25
Hard vacuum	Perlite	4	120	1.34	0.76	1.36
		3	118	1.23	0.79	1.20
		2 (long)	103	1.14	0.99	1.28
		2 (large)	437	2.28	0.64	3.31
		1	220	2.24	0.52	2.61
	MLI	4	87	1.28	0.71	1.16
		3	91	1.18	0.75	1.05
		2 (long)	83	1.10	0.95	1.16
		2 (large)	348	2.21	0.49	2.38
		1	193	2.20	0.48	2.32
	Aerogel beads	4	109	1.35	0.76	1.38
		3	110	1.23	0.80	1.21
		2 (long)	97	1.14	0.99	1.29
		2 (large)	409	2.29	0.65	3.42
		1	262	2.25	0.52	2.64

Table E.2: Tank integration characteristics for 345 kg mass of hydrogen

Vacuum level	Insulation material	Number of tanks	Total mass	Diameter of tank bundle	Length	Volume
No vacuum	Perlite	4	3960	2.85	5.99	48.57
		3	3179	2.31	6.05	32.34
		2 (long)	2740	2.00	7.44	29.78
		2 (large)	1828	2.86	4.59	37.56
		1	1224	2.72	3.78	27.90
	MLI	4	2029	2.45	5.71	34.31
		3	1669	2.03	5.80	23.83
		2 (long)	1465	1.77	7.21	22.69
		2 (large)	1138	2.69	4.26	30.89
		1	798	2.59	3.65	24.42
	Aerogel beads	4	1137	1.81	5.26	17.22
		3	972	1.56	5.40	13.22
		2 (long)	876	1.41	6.84	13.55
		2 (large)	820	2.42	3.72	21.87
		1	602	2.38	3.44	19.44
Soft vacuum	Perlite	4	2216	2.03	5.42	22.30
		3	1814	1.72	5.54	16.38
		2 (long)	1585	1.53	6.97	16.28
		2 (large)	1235	2.51	3.89	24.46
		1	857	2.44	3.50	20.80
	MLI	4	1116	1.74	5.22	15.86
		3	960	1.52	5.36	12.31
		2 (long)	869	1.37	6.80	12.72
		2 (large)	852	2.39	3.65	20.90
		1	627	2.35	3.42	18.81
	Aerogel beads	4	793	1.53	5.06	11.79
		3	709	1.36	5.23	9.66
		2 (long)	659	1.24	6.68	10.33
		2 (large)	739	2.30	3.48	18.44
		1	559	2.28	3.35	17.39
Hard vacuum	Perlite	4	521	1.32	4.92	8.56
		3	498	1.21	5.10	7.48
		2 (long)	481	1.13	6.56	8.33
		2 (large)	643	2.22	3.31	16.28
		1	501	2.21	3.28	16.10
	MLI	4	417	1.28	4.89	7.97
		3	417	1.18	5.07	7.07
		2 (long)	413	1.10	6.54	7.95
		2 (large)	606	2.20	3.27	15.86
		1	479	2.20	3.27	15.84
	Aerogel beads	4	488	1.32	4.92	8.62
		3	472	1.21	5.10	7.52
		2 (long)	460	1.13	6.57	8.37
		2 (large)	631	2.22	3.31	16.33
		1	484	2.22	3.28	16.13

Table E.3: Tank integration characteristics for 1000 kg mass of hydrogen

Vacuum level	Insulation material	Number of tanks	Total mass	Diameter of tank bundle	Length	Volume
No vacuum	Perlite	4	10985	2.81	15.24	120.14
		3	8761	2.28	15.63	81.29
		2 (long)	7649	1.98	19.83	77.86
		2 (large)	3146	2.68	10.43	74.73
		1	2802	2.64	9.92	69.22
	MLI	4	5642	2.42	14.96	87.75
		3	4614	2.00	15.39	61.73
		2 (long)	4100	1.76	19.61	60.70
		2 (large)	2082	2.56	10.19	66.59
		1	1882	2.53	9.80	62.79
	Aerogel beads	4	3173	1.80	14.52	46.86
		3	2699	1.55	15.00	36.22
		2 (long)	2461	1.40	19.25	37.76
		2 (large)	1591	2.36	9.80	54.70
		1	1457	2.35	9.62	53.19
Soft vacuum	Perlite	4	6133	2.01	14.67	59.28
		3	4991	1.70	15.13	43.96
		2 (long)	4422	1.52	19.37	44.71
		2 (large)	2227	2.42	9.91	57.87
		1	2005	2.40	9.67	55.68
	MLI	4	5911	2.38	14.94	84.78
		3	4812	1.97	15.36	59.65
		2 (long)	4263	1.73	19.58	58.69
		2 (large)	2181	2.53	10.13	64.64
		1	1963	2.50	9.77	61.09
	Aerogel beads	4	2218	1.52	14.33	33.10
		3	1977	1.35	14.83	27.20
		2 (long)	1856	1.24	19.09	29.38
		2 (large)	1490	2.27	9.62	49.69
		1	1375	2.27	9.54	49.03
Hard vacuum	Perlite	4	1470	1.32	14.18	24.65
		3	1400	1.21	14.70	21.54
		2 (long)	1365	1.13	18.97	24.05
		2 (large)	1348	2.21	9.50	46.54
		1	1254	2.21	9.49	46.43
	MLI	4	1182	1.28	14.15	23.08
		3	1178	1.18	14.68	20.46
		2 (long)	1175	1.10	18.95	23.03
		2 (large)	1293	2.20	9.48	45.91
		1	1207	2.20	9.47	45.90
	Aerogel beads	4	1378	1.32	14.19	24.83
		3	1329	1.21	14.71	21.66
		2 (long)	1304	1.13	18.98	24.17
		2 (large)	1330	2.21	9.50	46.61
		1	1249	2.21	9.49	46.49